UNIVERSITAT POLITÈCNICA DE CATALUNYA

MASTER THESIS

Effects of imperfections on the elastic properties of carbon nanotubes

Ignacio Valero Palacín

SUPERVISED BY

Ferhun C. Caner

Universitat Politècnica de Catalunya
Master in Aerospace Science & Technology
29th September 2009

Effects of imperfections on the elastic properties of carbon nanotubes

BY

Ignacio Valero Palacín

DIPLOMA THESIS FOR DEGREE

Master in Aerospace Science and Technology

AT

Universitat Politècnica de Catalunya

SUPERVISED BY:

Ferhun C. Caner

Institut de Tècniques Energètiques

ABSTRACT

Nanotubes are useful for not only strengthening polymer based materials that are of widespread use in aerospace applications, but also for their nondestructive testing. Nanotubes with defects are now routinely manufactured. Their manufacture without defects is still prohibitively expensive. Thus, it becomes important to be able to identify the defect percentage in the nanotubes, because the defects cause reduction in both strength and stiffness and electrical conductivity.

The elastic properties of carbon nanotubes with imperfections are studied using a model based on structural mechanics. The carbon - carbon bonds are modeled as load bearing beams joined together by the carbon atoms. The mechanical properties of a bond are obtained from a relationship between structural mechanics and molecular mechanics. The carbon nanotubes are drawn forming this structure and the stiffness matrix of the nanotube is obtained from the assembly of the stiffness matrix of each bond.

The obtained results for carbon nanotubes without imperfections are verified by comparing them to previous works. Furthermore, the number of degrees of freedom of each atom is reduced from six to three by neglecting the moments. This simplifies the model, reduces the computation time and allows the test of larger nanotubes with a low impact on the accuracy of the results.

Finally, different percentages of imperfections are introduced in the nanotubes in the form of missing atoms and the evolution of the Young's modulus with randomly imposed imperfection percentage is obtained. This relationship turned out to be almost linear when the imperfections percentage is small. The results obtained allow the prediction of the quality of carbon nanotubes from the elastic properties observed in experimental tests. If the Young's modulus of some nanotubes is found, then it can be directly related to a percentage of imperfections. The minimum number of necessary experimental tests to obtain statistically accurate results is also discussed.

ACKNOWLEDGEMENTS

I want to thank my supervisor, Ferhun Caner, for his dedication to this thesis. The time he devoted to the project, his implication and his knowledge were decisive to reach the results obtained. Thanks to his advice, I was able to work in some fields which were new for me and I have been able to learn a lot during our meetings.

Moreover, I express my gratitude to Ignasi Casanova, who introduced me in the world of nanotechnology. He gave me the opportunity to be in a stimulating research environment and advised me during all the process.

Finally, I thank my family, my girlfriend and my friends who supported and encouraged me during all the process that has led to this document.

Table of Contents

List of Figures

List of Tables

INTRODUCTION

Carbon nanotubes (CNT) are relatively young nanostructures. Despite the big research effort worldwide from its discovery in 1991, many of its properties are still under investigation.

CNTs are composed of carbon atoms arranged forming a cylindrical structure, similar to a rolled graphene sheet. This structure gives them unique properties which make this material attractive for a variety of applications. For example, CNTs have exceptional mechanical properties such as high stiffness and high strength.

These properties allow various applications of CNT in a wide variety of fields where the performance of the material or the device can be considerably improved by the introduction of carbon nanotubes. One of the main applications in the field of polymer composite materials is their reinforcement through the use of CNTs. The extraordinary mechanical properties of CNTs make them very suitable for design of materials with a high strength and a low weight. A material of these characteristics is necessary in the aerospace sector, where the compromise between strength and weight has always been a concern. Also, applications in the field of electronics are very promising as CNTs can act as a conductor or a semiconductor depending on its atomic configurations. Other aerospace applications include the fabrication of nano and micro electromechanical systems, sensors and thermal insulation.

The mechanical properties of CNTs can be determined both experimentally and through numerical simulations. Experimental measurements are normally performed using atomic force microscopy or electron microscopy. For the simulation of their mechanical behavior, there are more possibilities: from *ab initio* computations to quantum or molecular mechanics to classical mechanics.

In this thesis, an analysis method is developed to analyze the elastic behavior of CNTs. In particular, emphasis is placed on Young modulus of CNTs. The theory behind the simulations is based on structural mechanics. The base of the model is the stiffness matrix of a carbon – carbon bond, which is modeled as a cylindrical beam-column with 6 degrees of freedom defined between any two carbon atoms. The stiffness matrix of all beams is assembled into a global stiffness matrix forming the stiffness matrix for the whole nanotube.

The model allows application of various types of boundary conditions at the ends of the nanotube structure and extraction of results using the global stiffness matrix. Moreover, some bonds between atoms will be broken to study

the effect of imperfections in the form of atomic defects on the elastic properties.

The values of the structural mechanics parameters of the stiffness matrix of a single beam are determined by decomposing the bond energy obtained in molecular mechanics simulations to various deformation modes of a space frame element. These energy terms use force constants which are known, as they can be readily extracted from graphite.

The model will be tested in two versions: with six or three degrees of freedom per atom. Similar works have used six degrees but due to the weak torsional forces in a bond, but it will be shown that the simplifications will only have a minor influence on the accuracy of the results.

Once the elastic properties of the carbon nanotube have been successfully obtained for a given CNT, the method of analysis developed will be used to study the relation between the imperfections density in a CNT and the reduction in its Young’s modulus. Such a relation could be very useful to monitor the quality of CNTs using mechanical tests.

1 STATE OF THE ART

1.1 Carbon Nanotubes

1.1.1 Introduction

The basic crystalline forms of elemental carbon have been a well-known material for a long time. They have been used extensively across history in the forms of diamond, graphite and amorphous carbon.

Over the last twenty years, some new carbon atom arrangements have been discovered. In 1986, Kroto and Smalley [1] discovered the C60 molecule, also known as buckyball. This new form paved the way for a completely new class of carbon molecules: the fullerenes [2].

A wide variety of atom arrangements is made possible by the range of configurations of the electronic states of carbon atoms. The most common of these structures are shown in Fig. 1.1. The newest of them is the carbon nanotube (CNT), which was discovered by Iijima in 1991 [3]. However, this structure had already been observed by himself in 1979, when the first clear transmission electron microscopy (TEM) clear images were obtained [2,4].

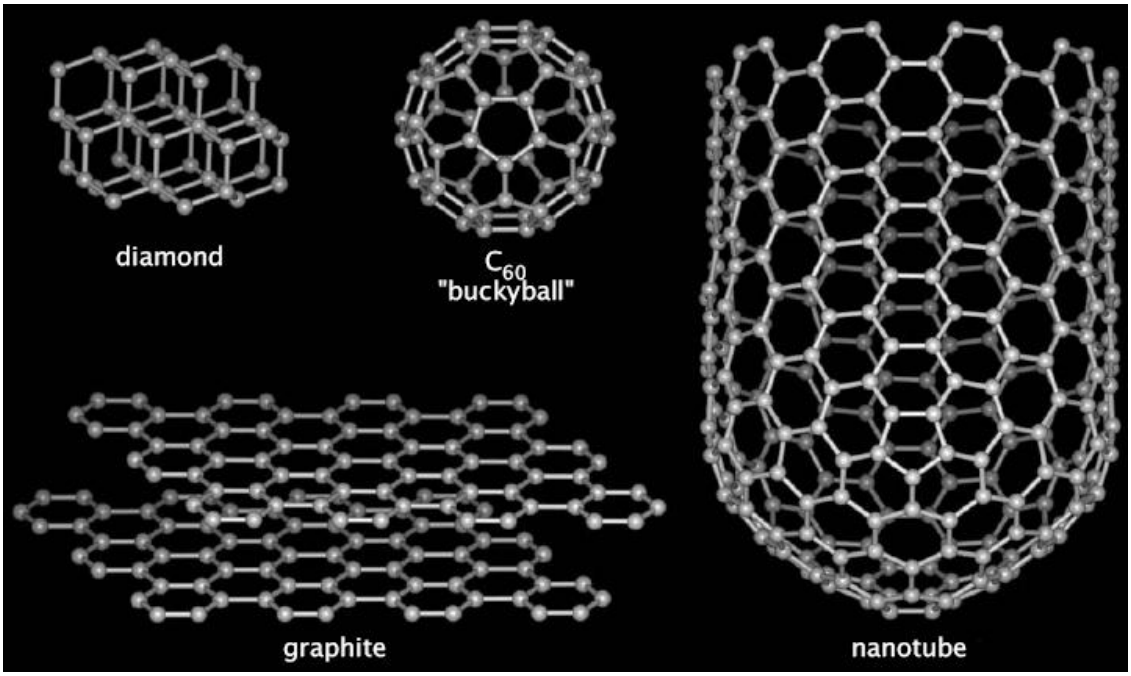

Fig. 1.1 Schematic representation of different types of fullerenes [5]

A single-wall carbon nanotube (SWCNT) can be defined by a hollow rolled cylindrical graphene sheet with a diameter of about 0.7-10 nm. However, most observed SWCNTs have diameters under 2 nm. There are also nanotubes with multi-walled structures, which will be discussed later. Nanotubes with lengths of several millimeters have already been obtained [6]. The aspect ratio (length/diameter) of this cylindrical structure can be as large as 10^4-10^5. Taking this into account and neglecting the two ends of the nanotube, we can consider it as a one-dimensional nanostructure [7].

Nanotubes have an exceptional combination of properties: small size, low density (similar to graphite), high stiffness, high strength and a variety of electronic properties. Such outstanding properties allow the application of CNTs in a wide range fields as reinforcing elements in high strength composites, electron sources in field emission displays and small X-ray sources, ultra-sharp and resistant atomic force microscopy (AFM) tips with high aspect ratios, gas sensors and components of future nanoscale electronics [2].

1.1.2 Structure

A nanotube is composed by carbon atoms forming six-membered carbon rings with the shape of a hexagon. The angle of this hexagon with the axis of the cylinder will determine the structure of the nanotube. Many possible structures exist as there are infinite angles in which a graphene sheet can be rolled into a SWCNT [7, 8].

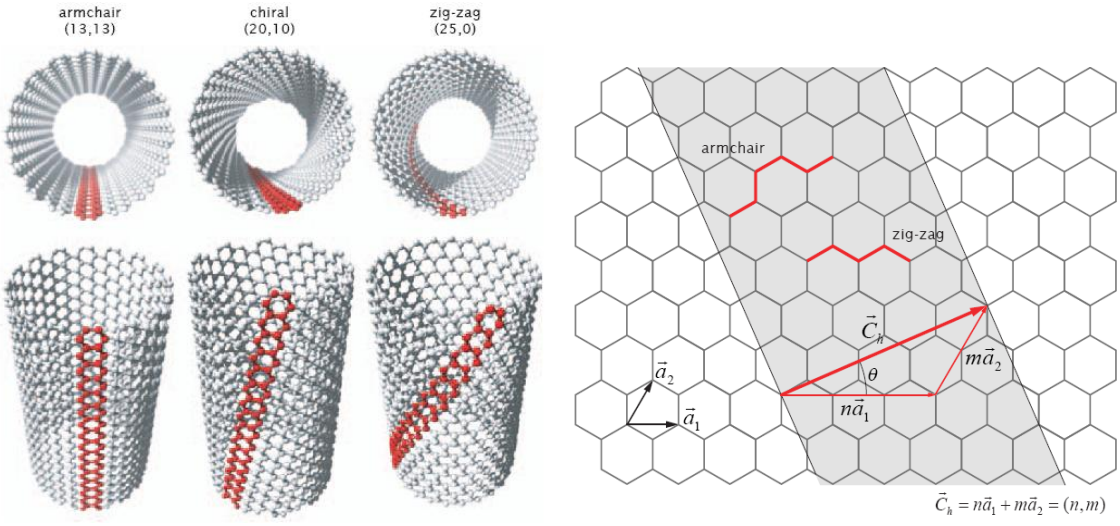

Fig. 1.2 Schematic illustrations of the structure of an armchair, chiral and zig-zag carbon nanotubes (right) and schematic diagram of nanotube formation by "rolling-up" a graphene sheet (right) [2]

Carbon nanotubes can be classified as achiral or chiral. The first type can be defined as a nanotube whose mirror image has the same structure as the original. There are two cases of achiral nanotubes: armchair and zigzag, which correspond to the first and third nanotube in Fig. 1.2. Their names come from the shape of their cross-sectional ring, as shown in the scheme at the right of the same figure. Nanotubes whose mirror image is different to the original are called chiral [7].

These structure variations can be cataloged according to the chiral vector or chiral angle θ. Fig. 1.2 shows a graphene sheet and the unit vectors that will determine the chirality. According to that, the chiral vector is:

$$C_h = n\bar{a}_1 + m\bar{a}_2 = (n, m) \quad \textbf{(1.1)}$$

The twist that the angle θ determines is clearly shown in Fig. 1.2. The extreme cases are θ=0° for the armchair configuration and θ=30° for a zigzag carbon nanotube. The angles in between correspond to chiral CNTs [2].

The importance of this issue is due to the fact that it determines some properties of the carbon nanotube, especially the conductivity [9]. Graphite is considered to be a semi-metal, but it has been shown that, depending on tube chirality, nanotubes can be either metallic or semiconducting [10].

Carbon nanotubes can be single-walled or multi-walled (SWCNT and MWCNT respectively). SWCNT have already been defined. A MWCNT consists of multiple rolled layers of graphite which can be seen as concentric single-walled tubes. The distance between layers in MWCNTs is similar to the distance between graphene layers in graphite, approximately 3.3 Å. There is an intermediate case, which is called double-walled carbon nanotubes (DWCNT).

The mechanical and chemical properties of each type of CNT are slightly different. Moreover, the nanotube surface can be chemically modified to, for instance, improve the adhesion to a polymer matrix. Fig. 1.3 exemplifies the wide range of possible structures of a carbon nanotube, including the number of walls, type of functionalization, etc. From this work, it can be seen that strengthening of a polymer due to CNT increases as diameter decreases but single-walled CNT are inefficient as there are prone to bundle formation [11].

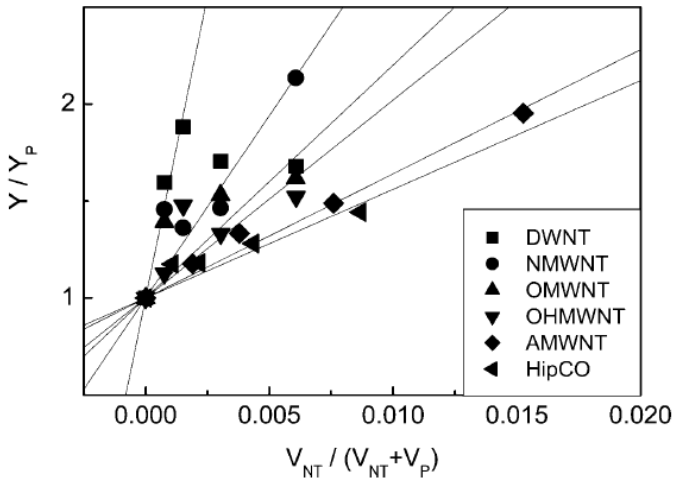

Fig. 1.3. Young modulus versus nanotubes volume fraction for each composite film. NMWNT and OMWNT: catalytic MWCNT, AMWNT: arc grown MWNT, OHMWNT: functionalized MWCNT, HipCO: SWCNT [11]

1.2 Study of mechanical properties

1.2.1 Introduction

Two different theoretical approaches can be followed to estimate the mechanical properties of carbon nanotubes: bottom up or top down. Bottom up methods are based on quantum on molecular mechanics including the classical molecular dynamics (MD) and *ab initio* methods. Top down approaches are mainly based on continuum mechanics. The most accurate results are obtained by *ab initio* methods, though they are extremely expensive computationally. They can only be used in very small systems with a maximum of a few hundreds of atoms. Despite the computational power increases, classical molecular dynamics simulations are still limited to the order of 10^6–10^8 atoms for a few nanoseconds. The simulation of larger systems or during a longer period can only be performed through continuum mechanics approaches. However, theories for describing continuum materials at the nanoscale have reached their limit and their accuracy becomes questionable [12].

1.2.2 Molecular dynamics

In the field of molecular dynamics, a carbon nanotube can be considered as a group of carbon atoms which form a carbon molecule. Each atom nucleus can be regarded as a single material point. The movements of these atoms are modeled by a force field formed by the interactions between nuclei and between nucleus and electrons. This force field is expressed by a potential energy and

only depends on the relative position to other atom nuclei of the molecule. The general expression of this potential energy, if electrostatic interaction is neglected, is:

$$U=\sum Ur+\sum U\theta+\sum U\varphi+\sum U\omega+\sum Uvdw+\sum Ues, \quad \textbf{(1.2)}$$

where Ur is for bond stretching energy, U_θ is for angle variation energy, U_φ is for the dihedral angle torsion energy, U_ω is for the inversion (also known as out of plane torsion) energy, U_{vdw} and U_{es} are for non-bonding energies (van der Waals and electrostatic interaction respectively). Each of these energies is represented in the schematic illustration of a bond structure in Fig. 1.4**.** Additionally, terms associated to electromechanical or optomechanical interactions can be likewise included. In covalent systems, such as carbon nanotubes, the main contributors to the potential energy are the first four terms [13, 14, 15].

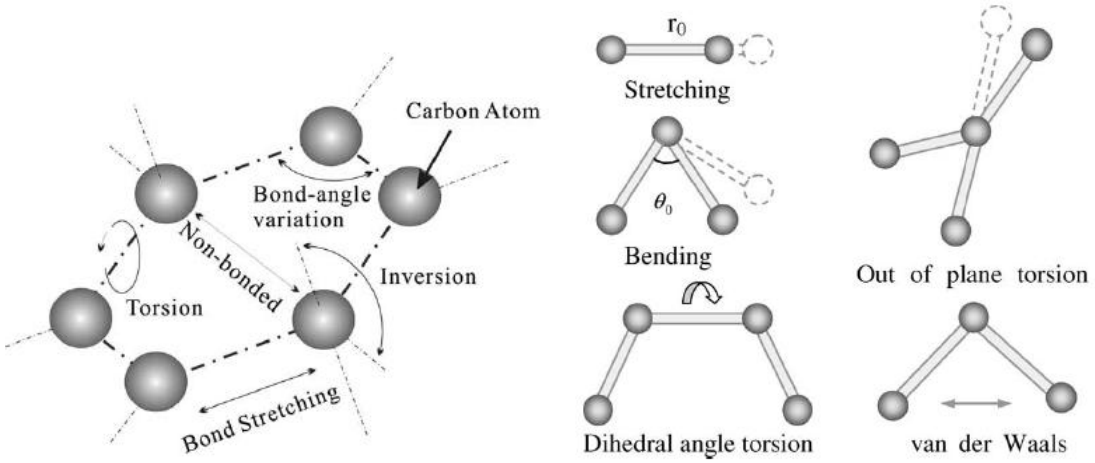

Fig. 1.4 Bond structures and corresponding energy terms of a graphene cell (left) [14] and interatomic interactions in molecular mechanics (right) [13]

[↓Chang2003] There is a large amount of literature about finding a reasonable functional form to define each of these potential energy terms. Hence, many forms can be used for each term, depending on the particular material and the loading conditions. If a small deformation is assumed, a harmonic approximation can be used to describe this energy. Chemical calculations have shown that these functions provide a reasonable approximation. In particular, the bond stretching energy is written as

$$U_r = \frac{1}{2}\sum_i k_{r_i}(dr_i)^2 \quad \textbf{(1.3)}$$

where dr_i is the elongation of bond i and k_{ri} is a force constant which is different for every material and is associated with bond stretching.

In a similar way, angle variation and inversion energies can be described as

$$U_\theta = \frac{1}{2}\sum_j k_{\theta_j}\left(d\theta_j\right)^2 \quad \textbf{(1.4)}$$

$$U_\omega = \frac{1}{2}\sum_k k_{\omega_k}(d\omega_k)^2 \quad \textbf{(1.5)}$$

where $d\theta_j$ and $d\omega_k$ are the change of bond angle j and inversion angle k, $k_{\theta j}$ and $k_{\omega k}$ are force constants which are different for every material and are associated with angle variance and inversion, respectively.

In molecular mechanics, the dihedral angle torsion energy is mainly used for the correction of the other bonded energy terms rather than to reflect an existing physical process. Hence, the torsional potential is not always present in a molecular mechanics force field. Its utilization is, in general, limited to the cases where it is necessary to adjust the total energy of the system in order to achieve a desired energy profile. The potential representing the dihedral angle torsion energy is usually modeled by a periodic function like a cosine series expansion:

$$U_\phi = \frac{1}{2}\sum_i k_{\phi_i}[1 + cos(n_i\tau_i - \phi_i)] \quad \textbf{(1.6)}$$

where $k_{\phi i}$ is the 'barrier' height to rotation of the bond i; n_i is multiplicity which gives the number of minima as the bond is rotated through 2π.

For simplicity and convenience, the dihedral angle torsion and the out of plane torsion energies can be merged into an equivalent term [13]:

$$U_\tau = U_\phi + U_\omega = \frac{1}{2}\sum_i k_{\tau_i}(d\phi_i)^2 \quad \textbf{(1.7)}$$

where U_τ is the torsion energy, $k_{\tau i}$ is the torsional resistance constant and $d\phi_i$ is the twist angle for the bond i.

Non-bonding energies are used to model the interactions between a couple of atoms which not necessarily has a bond in common. These forces are normally divided into two categories: van der Waals interaction and electrostatic

interaction. For the first one, the Lennard–Jones potential is used. This is a widely known empirical function with the following form:

$$U_{vdW} = \sum_{i,j} e_{i,j} \left[\left(\tilde{r}_{i,j} / r_{i,j} \right)^{12} - 2 \left(\tilde{r}_{i,j} / r_{i,j} \right)^{6} \right] \quad \textbf{(1.8)}$$

where e_{ij} is the potential well depth, $\tilde{r}_{ij}$ is the reference distance above which atoms i and j can interact and r_{ij} is the separation between atom i and atom j. The other non-boding energy, electrostatic interaction, can be described by Coulomb's law as

$$U_{es} = \sum_{i,j} {kq_i q_j} \Big/ {r_{ij}} \quad \textbf{(1.9)}$$

where k is Coulomb's constant, r_{ij} is the distance between atoms i and j, and q_i and q_j are point charge of atoms i and j, respectively [15].

One of the main advantages of this formulation of a carbon nanotube using molecular mechanics is that the total potential energy of the system is fragmented into individual terms and each one has its physical meaning. This formulation also allows neglecting or focusing in one or some of the terms to study a specific problem. For example, in order to determine the tensile modulus of a single-walled nanotube subjected to uniaxial loadings, it is not necessary to take into consideration all the terms, so the problem can be simplified. It can be observed that at small deformations, energy terms for interactions due to torsion, inversion, van der Waals forces, and electrostatic forces are small compared with the terms due to bond stretching and angle variation. Therefore, the total energy of the single-walled nanotube can be reduced to [15, 16]:

$$U_{total} = \frac{1}{2} \sum_i k_{r_i} (dr_i)^2 + \frac{1}{2} \sum_j k_{\theta_j} \left(d\theta_j \right)^2 \quad \textbf{(1.10)}$$

1.2.3 Structural mechanics

The carbon atoms of a nanotube are bonded between them by covalent bonds forming a hexagonal pattern. The bonds have known characteristic bond lengths and angles. If an external force is applied to the nanotube, these bonds constrain the displacement of the atoms. Hence the total displacement of the nanotube is a result from the interactions between these bonds.

The structural mechanics approach considers the covalent bonds as connecting elements between carbon atoms, which act as a joint of three elements. Hence a SWCNT can be simulated as a space frame-like structure.

A relation between the parameters used in structural mechanics and molecular mechanics, sectional stiffness and force constants respectively, can be set as follows. The bond between every two carbon atoms will be considered as identical, and cylindrical. Then $I_x=I_y=I$ can be assumed and thus three stiffness parameters should be determined.

To obtain the sectional stiffness parameters, the strain energies of structural elements will be considered. They will be found under individual forces, in the same way that the energy terms in molecular mechanics stand for single interaction and the effects of cross interactions are not included. These energies can be easily obtained from classical structural mechanics.

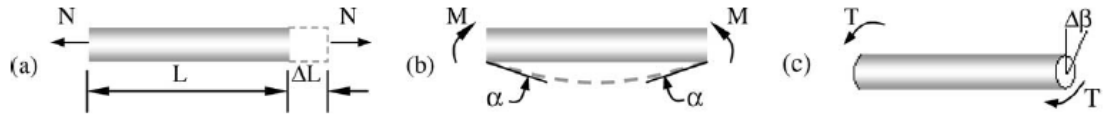

Fig. 1.5 Pure tension, bending and torsion of an element [13]

For a uniform beam subjected as in Fig. 1.5a to a pure axial force, its strain energy is

$$U_A = {}^1\!/_2 \int_0^L \left({}^{N^2}\!/_{EA} \right) dL = {}^1\!/_2 \, {}^{N^2 L}\!/_{EA} = {}^1\!/_2 \, {}^{EA}\!/_L \, (\Delta L)^2 \qquad \textbf{(1.11)}$$

where L is the length of the beam, N is the force exerted and ΔL is the axial stretching deformation. The strain energy for the same beam if a pure bending moment is exerted (Fig. 1.5b) is

$$U_M = {}^1\!/_2 \int_0^L \left({}^{M^2}\!/_{EI} \right) dL = \left({}^{2EI}\!/_L \right) \alpha^2 = {}^1\!/_2 \, {}^{EI}\!/_L \, (2\alpha)^2 \qquad \textbf{(1.12)}$$

where M is the bending moment and α is the rotational angle at each extreme of the beam. For this beam, the strain energy under pure torsion (Fig. 1.5c) can be written as

$$U_T = {}^1\!/_2 \int_0^L \left({}^{T^2}\!/_{GJ} \right) dL = {}^1\!/_2 \, {}^{T^2 L}\!/_{GJ} = {}^1\!/_2 \, {}^{GJ}\!/_L \, (\Delta\beta)^2 \qquad \textbf{(1.13)}$$

where T denotes the torsion applied and Δβ is the relative rotation between the ends of the beam.

From the previous equations, it can be seen that U_r and U_A are equivalent. The same happens with U_θ and U_M and with U_τ and U_T. They represent stretching energy, bending energy and torsional energy, respectively. The rotation of angle 2α can be assumed as the same as the total bond angle change Δ_θ. Likewise, the equivalence between Δ_L and δ_r for the bond stretching, and Δ_β and δ_ϕ for the bond twist angle can be established.

Therefore, if equations 1.2, 1.3 and 1.7 are compared with equations 1.11, 1.12 and 1.13 a relationship between the parameters in molecular mechanics and the ones in structural mechanics can be obtained as follows:

$$ {}^{EA}\!/_L = k_r, \quad {}^{EI}\!/_L = k_\theta, \quad {}^{GJ}\!/_L = k_\tau \qquad \textbf{(1.14)}$$

The force constants are known and can be easily found in the literature, so the stiffness parameters EA, EI and GJ can be obtained. These expressions are the base to the application of the theory of structural mechanics in order to model fullerene structures such as carbon nanotubes [13].

1.2.4 Experimental Methods

The mechanical characterization of nanopartícules is complex due to the high resolutions needed: nanoNewtons and nanometers or better. The experimental techniques already developed can be divided into two categories: nanoindentation/ atomic force microscopy (AFM) testing and *in-situ* electron microscopy.

The first category uses instruments which are commercially available to apply a load a measure at the same time the resulting deformation. It uses a nanoindenter (an instrument that monitors load and position) and an AFM (an instrument designed to obtain 3D topographical images with a high resolution), which in this case will be used to deflect de tip of the nanotube. There are different modes of operation for an AFM: lateral mode, contact mode and force microscopy mode. Schemes of their operation are shown in Fig. 1.6. Those

methods have a high resolution and reliability and the preparation is quite simple. However sample imaging during the test cannot be achieved [17].

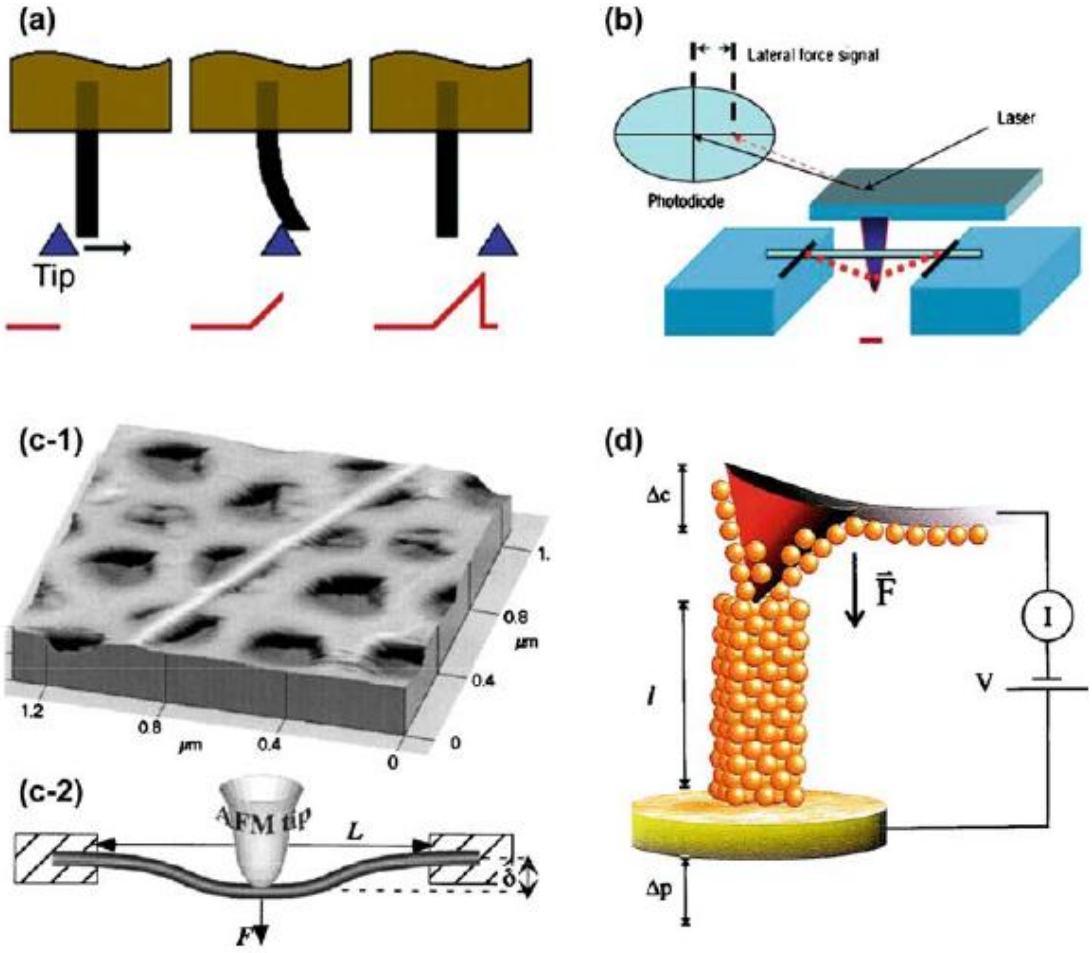

Fig. 1.6 (a) A cantilever nanotube deflected by an AFM in the lateral mode. (b) A double-clamped nanowire deflected horizontally by an AFM in the lateral force mode. (c-1) A MWCNT suspended over a porous alumina membrane; (c-2) The MWCNT deflected vertically by an AFM in the contact mode. (d) A gold nanowire stretched by an AFM in force microscopy mode [17]

In the second category of experimental characterization, a deformation and a load are imposed using piezoactuators or two AFM. The process is imaged through in-situ Scanning Electron Microscopy (SEM) and/or Transmission Electron Microscopy (TEM). The measure of deformation is taken from the obtained images. Load sensing must be performed independently, which is usually achieved by SEM or TEM imaging of a flexible member attached to the sample in series [17].

1.3 Mechanical properties

Carbon nanotube is widely recognized as one of the strongest materials in the world. This statement is based in a wide variety of simulations and experimental measurements. Although they are currently used as a reinforcement filler for polymers, among many other applications in a variety of fields, their true mechanical properties such as the Young's modulus, elastic properties, yield strength, ultimate strength and fracture behavior are not well known yet and need further study.

According to experiments to this date, Young's moduli of carbon nanotubes range from 270 to 950 GPa. The reason for such a large discrepancy is that tested CNT had different sizes, lengths and numbers of wall layers. This is a difficulty which is hard to overcome as it is very complicated to produce identical nanotubes, even in the same experiment. Fig. 1.7 shows a tensile test for a multi-walled CNT.

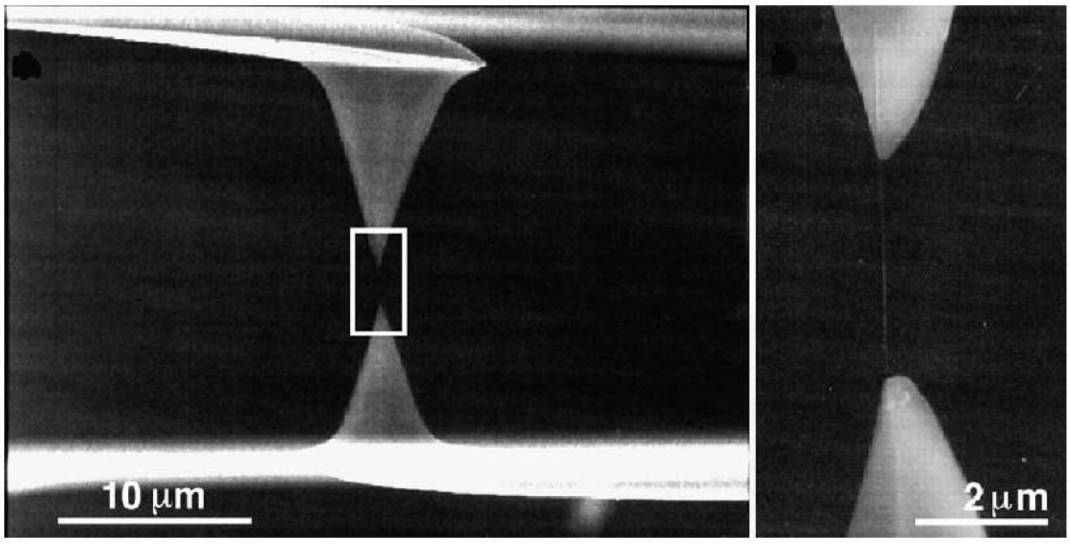

Fig. 1.7 Tensile strength test of multi-walled nanotube [18]

In multi-walled carbon nanotubes, their inner layers do not receive the tensile loads applied at both ends. This happens due to the weak stress transferability between the layers of the nanotube. Hence, load is taken almost entirely by the outmost layer. Therefore, the failure of a multi-walled carbon nanotube will start at the outmost layer with the breakage of the bonds between atoms of carbon [18].

The effect of the geometrical morphology and structure of nanotube (diameter, length, number of walls) on the mechanical properties have not been well established yet. Often substrates remain inside the nanotubes and contaminate

the results of the tests which investigate in this direction [18]. Table 1.1 shows Young's moduli of CNT by several different methods, including molecular dynamics (MD), finite element methods (FEM), theoretical calculations and experimental tests. The large variation in results may be due to the variations of bulk materials and the nanotubes purification [16].

Table 1.1 Comparison of the Young's moduli of carbon nanotubes by previous studies [16]

Authors	E (TPa)	ν	Year	Method
Yakobson	5.5	0.19	1996	MD
Zhou et al.	0.77	0.32	2001	Theoretical
Lu	1.0	0.28	1997	MD
Tu	4.7	0.34	2002	Theoretical
Chang and Gao	1.325	0.26	2003	MD
Krishnan et al.	1.25	-	1998	Theoretical
Li and Chou	1.05	-	2003	FEM
Yu et al.	0.27-0.95	-	2000	Experimental
Li et al.	0.79	-	2000	Experimental
Demczyk et al.	0.9	–	2002	Experimental

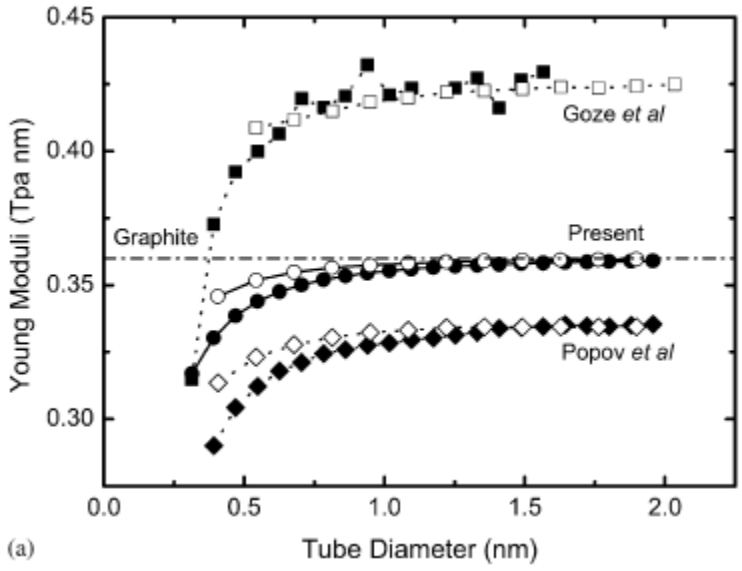

Fig. 1.8 Comparison between the predictions from the present model with existing results on the size-dependence of Young's modulus. Open symbols stand for armchair tubes and solid symbols for zigzag tubes [15]

The diameter of the nanotube also affects its mechanical properties. Models have been elaborated by some researchers [15, 19, 20] with similar results about size-dependence. For small diameters, Young modulus increases with the diameter up to a value (see Fig. 1.8). At this value, which varies from a model to another, the modulus becomes independent of size and does not increase anymore.

1.4 Aerospace applications

The fibrous structure of carbon nanotubes, their low density, the high aspect ratio and the extraordinary mechanical properties make them especially attractive to reinforce polymer composite materials [21]. It is widely known that one of the keys concepts in the design of aeronautical or aerospace structures is low weight at the same time high stiffness and strength. Over the last years, a transition from metals to carbon-fiber reinforced composites in aircrafts has taken place precisely to increase the stiffness and strength while reducing the self weight of the aircraft. It is likely that, a low density strong material such as CNT, fulfills the requirements to be used in nanocomposites and allow the evolution of aerospace materials. As an example of the exceptional properties of nanocomposites, Dalton et al. [21] fabricated a few hundreds of meters of composite fibers of poly(alcohol vinyl) with a 60% wt of single-walled carbon nanotubes. This resulted in a material with a tensile strength of 1.8 GPa, comparable to spider silk.

Strengthening of materials is not the only field in which carbon nanotubes can be used. The high conductivity of a carbon nanotube can reduce the resistivity of a polymer in many orders of magnitude. These increases have been measured with concentrations of SWCNTs under 0.1% in weight. Moreover the mechanical or optical properties of the composite are maintained or even increased, as previously explained. There is a wide range of applications for these improved electrical properties, such as electrostatic dissipation, electrostatic painting, electromagnetic interference shielding, conductive transparent coatings or embedded sensors [22, 23].

Another application of CNT is to improve thermal properties of the materials. This can be particularly interesting in aerospace applications, where the spacecrafts must support extreme conditions. It has been demonstrated that CNT reduce considerably the flammability of the composite where they are used, especially if they are single-walled [24]. Of course, the applicability of these advantages to the field of aeronautics is also clear. Finally, there is also a wide range of applications of CNT for electronics, as they can also act as semiconductors.

2 METHODOLOGY

2.1 Visualizing the nanotube

The first step in modeling the nanotube is visualizing it using the coordinates of its atoms.

The first step of this process will be done using *Nanotube Modeller*, a computer program developed by JCrystalSoft that can generate xyz-coordinates for nanotubes and nanocones in a wide variety of conditions. The limited version of this program available online can show the coordinates and the image of a nanotube but cannot export them. Hence, only a ring of the nanotube structure is created, so that the nanotube can be later reproduced by the repetition of this basic structure as shown in Fig. 2.1.

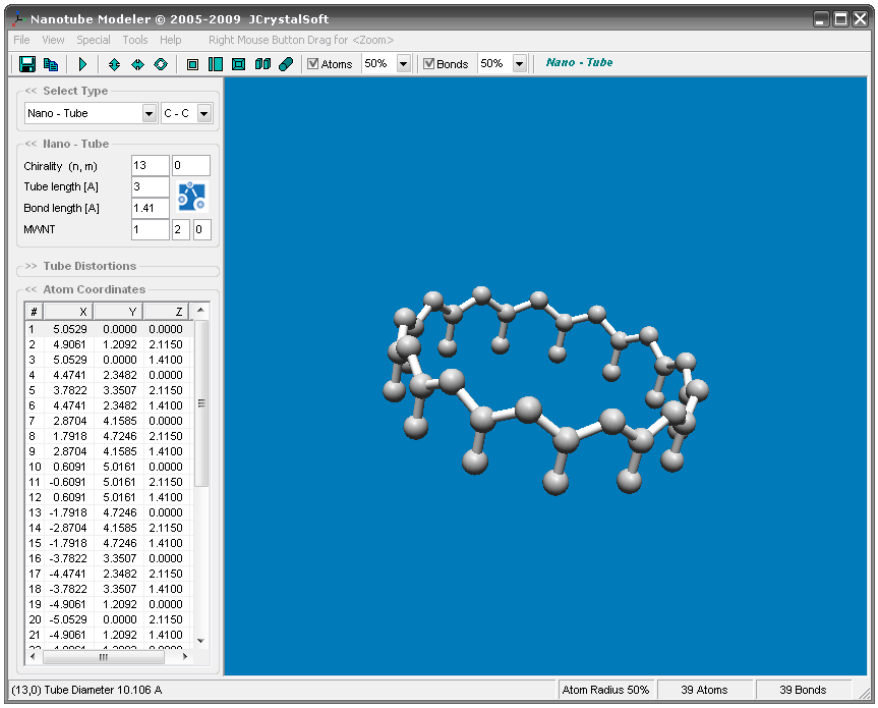

Fig. 2.1 Fragment of a carbon nanotube created with *Nanotube Modeller*. The coordinates of the atoms appear in the lower left corner of the screen.

Next, the coordinates obtained are manually introduced into *GiD*, a computer program developed by CIMNE (International Center for Numerical Methods in Engineering) at UPC. With this program, it is possible to draw geometrical models and create meshes, which can later be exported in several formats to perform finite element analysis calculations.

Once the points corresponding to the atoms have been manually introduced into GiD, the mesh is obtained by joining the adjacent atoms by lines that represent beam elements (Fig. 2.2a). Then this fragment of nanotube is copied (Fig. 2.2b) and rotated (Fig. 2.2c) to form a structure that can be repeated without further changes to obtain the desired length of the nanotube (Fig. 2.2d). During the process of copying the successive rings to form the tube, in some cases, several nodes may get created twice, which after meshing leads to errors in the computations. Thus, duplicate nodes were carefully determined and eliminated.

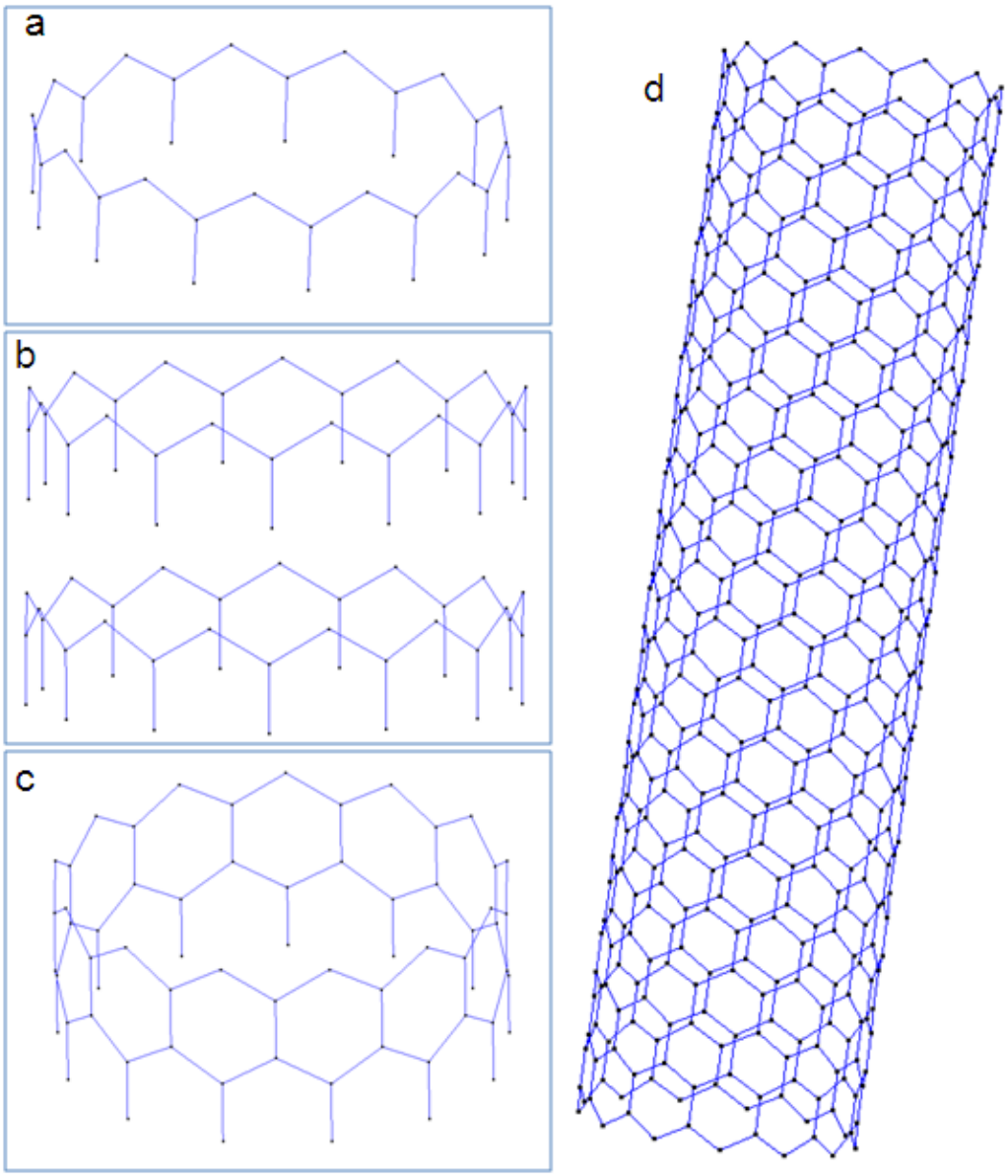

Fig. 2.2 Screenshots of the process of creating a carbon nanotube in GiD.

Once the geometry is ready, the mesh is created and exported. The format selected is a GiD mesh file, which lists the coordinates of all the nodes and then lists the nodes connected by each element.

The model to find the mechanical properties of the created nanotube was written and executed using Matlab. Thus, the output mesh file has to be converted into a format that is accepted by Matlab. The most convenient way was to transfer the data to a Microsoft Excel table. This step was also used to eliminate information about the mesh that was unnecessary for the model and to divide the information on two files: one for the elements and other for the nodes. Then each table could be exported to Matlab and saved in the file format of this program (*.mat).

As a result of all this process, two files contain all the data of the nanotube structure and are ready to be used as the input to the program that will be explained in the following sections. The first file is a list of all the nodes in the nanotube, with their three coordinates. The second one is a connectivity matrix, that is to say, a list of all elements together with the number of the nodes at each end.

2.2 Bond stiffness

The basis of the entire model is the stiffness matrix of a bond between two carbon atoms. This matrix is used to assemble it in the system stiffness matrix, which represents the stiffness of the whole nanotube.

The bond is considered as a beam element as shown in Fig. 2.3. Each element will have twelve degrees of freedom, six at each end. Namely, there will be three for the deformations in each direction and another three for the angle variations.

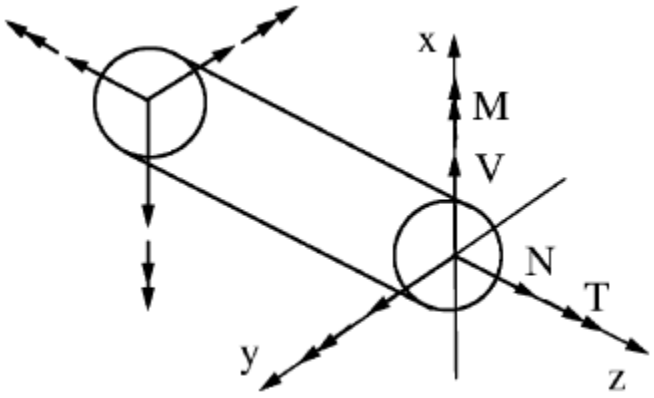

Fig. 2.3 Illustration of a beam element in a space frame [13]

For any element, the elemental equilibrium equation can be written as:

$$K \cdot u = f \tag{2.1}$$

where

$$u = \left[u_{xi}, u_{yi}, u_{zi}, \theta_{xi}, \theta_{yi}, \theta_{zi}, u_{xj}, u_{yj}, u_{zj}, \theta_{xi}, \theta_{xj}, \theta_{xz}\right]^T \tag{2.2}$$

$$f = \left[f_{xi}, f_{yi}, f_{zi}, m_{xi}, m_{yi}, m_{zi}, f_{xj}, f_{yj}, f_{zj}, m_{xi}, m_{xj}, m_{xz}\right]^T \tag{2.3}$$

are vectors of displacements and forces, respectively at each node. As previously stated, each vector includes the linear and angular energetically conjugate magnitudes. K_i in equation 2.1 corresponds to the stiffness matrix of the beam element, which, for simplicity can be divided into four sub-matrices:

$$K_i = \begin{bmatrix} K_{ii} & K_{ij} \\ K_{ij} & K_{jj} \end{bmatrix} \tag{2.4}$$

where

$$K_{ii} = \begin{bmatrix} EA/L & 0 & 0 & 0 & 0 & 0 \\ 0 & 12EI/L^3 & 0 & 0 & 0 & 6EI/L^2 \\ 0 & 0 & 12EI/L^3 & 0 & -6EI/L^2 & 0 \\ 0 & 0 & 0 & GJ/L & 0 & 0 \\ 0 & 0 & -6EI/L^2 & 0 & 4EI/L & 0 \\ 0 & 6EI/L^2 & 0 & 0 & 0 & 4EI/L \end{bmatrix} \tag{2.5}$$

$$K_{ij} = \begin{bmatrix} -EA/L & 0 & 0 & 0 & 0 & 0 \\ 0 & -12EI/L^3 & 0 & 0 & 0 & 6EI/L^2 \\ 0 & 0 & -12EI/L^3 & 0 & -6EI/L^2 & 0 \\ 0 & 0 & 0 & -GJ/L & 0 & 0 \\ 0 & 0 & 6EI/L^2 & 0 & 2EI/L & 0 \\ 0 & -6EI/L^2 & 0 & 0 & 0 & 2EI/L \end{bmatrix} \tag{2.6}$$

$$K_{jj} = \begin{bmatrix} EA/L & 0 & 0 & 0 & 0 & 0 \\ 0 & 12EI/L^3 & 0 & 0 & 0 & -6EI/L^2 \\ 0 & 0 & 12EI/L^3 & 0 & 6EI/L^2 & 0 \\ 0 & 0 & 0 & GJ/L & 0 & 0 \\ 0 & 0 & 6EI/L^2 & 0 & 4EI/L & 0 \\ 0 & -6EI/L^2 & 0 & 0 & 0 & 4EI/L \end{bmatrix} \quad \textbf{(2.7)}$$

In theses matrices, there are several different parameters, but the values of all of them are known or can be easily obtained. In the foregoing equations, the length of a bond between carbon atoms is assumed to be L=0.141 nm; EA is the tensile resistance; EI is the flexural rigidity and GJ is the torsional stiffness [13].

2.3 Matrix assembly

The first step to assembly the stiffness matrix of each element into the structural stiffness matrix is to transform the element stiffness matrices from local to global coordinates. To do this, the position and orientation of each element should be determined.

To determine the angle between the directions in the global coordinates and for each local element, the file with the coordinates of the nodes is used. The vector corresponding to the axial direction of any given element can be determined as

$$u_z = (a_x - b_x, a_y - b_y, a_z - b_z) \quad \textbf{(2.8)}$$

where a_x, a_y and a_z are the coordinates for the node at one end and b_x, b_y and b_z are the coordinates of the node at the other end of the element. The unit vector in the axial direction of any given element is obtained by normalizing the above vector.

Then, the two other directions need to be determined. As the beam element is assumed to be cylindrical, the two other directions can be chosen arbitrarily, as long as they form a mutually orthogonal system of coordinates. Also further calculations will have to be consistent with this choice.

There are infinitely many vectors perpendicular to the axial direction. Hence, two of the three components of the vector Y must be constrained and third one needs be found. As the principle to follow is the perpendicularity of the axes, the following expression, corresponding to the dot product of two vectors must be used:

$$y_1 z_1 + y_2 z_2 + y_3 z_3 = 0 \quad \textbf{(2.9)}$$

In the above equation, y_1, y_2, and y_3 are the components of the vector $\overrightarrow{u_y}$ in the direction of the Y axis and z_1, z_2 and z_3 are for the vector $\overrightarrow{u_z}$ in the Z axis. The data for the vector $\overrightarrow{u_z}$ is already available and y_1 and y_2 will be set to arbitrary but different numbers such as 1 and 2 respectively. Then, the components of the Y axis will be (1, 2,y_3), where y_3 can now be obtained using the above equation.

Now it is straight forward to obtain the components of the vector in the direction of the X axis. It should be perpendicular to the previous two so the cross product of the previous two will be calculated:

$$\overrightarrow{u_x} = \overrightarrow{u_y} \times \overrightarrow{u_z} \quad \textbf{(2.10)}$$

Then, once the vectors for the local coordinates have been obtained and normalized, the angle between them and the global axes can be found. Using again the dot product of two vectors in the following form:

$$\overrightarrow{v_1} \cdot \overrightarrow{v_2} = |v_1||v_2| \cos\theta \quad \textbf{(2.11)}$$

where v_1 and v_2 are two given vectors and θ is the angle between them.

Assuming that all vectors are unit vectors, the expression is simplified. Now, the angle between each local vector to each global vector can be found. For example, the cosine of the angle between the local axis Z and the global axis X (θ_{zi}) is:

$$\cos\theta_{zi} = \overrightarrow{u_z} \cdot \hat{\imath} \quad \textbf{(2.12)}$$

where $\hat{\imath}$ is a unit vector in the direction of the global X axis. Thus, its components are (1, 0, 0). In the same way, the vectors $\hat{\jmath}$ and $\hat{k}$ will also be created and will correspond to the Y and Z axes respectively.

These cosines of the angles can be used to rotate the stiffness matrix from the local to the global coordinates. To achieve that, the following operation should be performed:

$$K_{i,global} = R^T \cdot K_{i,local} \cdot R \quad \textbf{(2.13)}$$

where $K_{i,local}$ is the stiffness matrix for a bond element (from Eq. 2.4), $K_{i,global}$ is the same matrix but transformed into the global coordinates and R is:

$$R = \begin{bmatrix} R_S & R_0 & R_0 & R_0 \\ R_0 & R_S & R_0 & R_0 \\ R_0 & R_0 & R_S & R_0 \\ R_0 & R_0 & R_0 & R_S \end{bmatrix} \quad \textbf{(2.14)}$$

where R_S and R_0 are:

$$R_S = \begin{bmatrix} cos\,\theta_{zi} & cos\,\theta_{zj} & cos\,\theta_{zk} \\ cos\,\theta_{yi} & cos\,\theta_{yj} & cos\,\theta_{yk} \\ cos\,\theta_{xi} & cos\,\theta_{xj} & cos\,\theta_{xk} \end{bmatrix} \quad \textbf{(2.15)}$$

$$R_0 = \begin{bmatrix} 0 & 0 & 0 \\ 0 & 0 & 0 \\ 0 & 0 & 0 \end{bmatrix} \quad \textbf{(2.16)}$$

The rotation matrix is symmetric and the non-zero matrix is repetitive as the forces and the moments share the same axes. Hence, the rotation angles previously found are valid for forces and moments at both ends.

At this point, the stiffness matrix of a beam element that corresponds to the bond between two atoms is in accordance with the global coordinates of all the nanotube. The next step is to assemble it into the global stiffness matrix. This will be a large sparse square matrix with the total number of rows and columns equal to the number of atoms times the degrees of freedom at each atom. For example, for a nanotube with a diameter of 1 nm, with 494 atoms and 6 degrees of freedom for each of them, the size of the matrix will be 2964 x 2964.

The assembly of the global stiffness matrix is performed as shown in Fig. 2.4, in which element stiffness matrix components for each element is added to the right components in the global stiffness matrix using the connectivity matrix of the elements.

The process described in this section will be repeated for each element of the nanotube. At the end of the loop, the contribution of each bond element to the stiffness matrix K is accumulated and finally when all elements are processed, the global stiffness matrix is obtained.

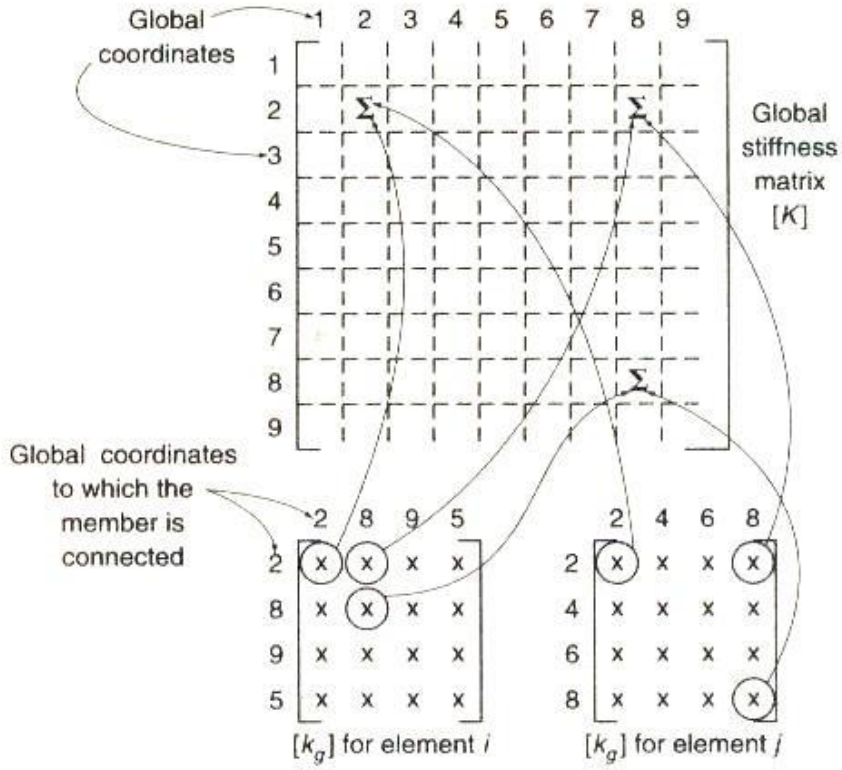

Fig. 2.4 Scheme of the process to assemble element matrices into the global matrix [25]

The process described in this section will be repeated for each element of the nanotube. At the end of the loop, the contribution of each bond element to the stiffness matrix K is accumulated and finally when all elements are processed, the global stiffness matrix is obtained.

2.4 Obtaining results

To obtain the Young's modulus of the modeled carbon nanotube it is necessary to apply a given force to the structure and then calculate the resulting deformation using the stiffness matrix or vice versa. As shown in Fig. 2.5, a force (F) or a displacement (u) will be applied to one of the ends of the CNT and the other end will be fixed.

When displacement is applied to each of the atoms at the end of the nanotube, the sum of all the corresponding forces (reactions) will be the total force used. When forces are applied at each atom, the displacements are obtained by solving the linear system of equations.

Fig. 2.5 Scheme of the forces applied to the carbon nanotube

There are two different paths that can be followed in order to apply these force or displacements and do the calculations, which imply the use of very large matrices to solve the equation F=K·u.

The first way that was used in the code was to divide the two vectors (F and u) and the matrix (K) into parts, as shown in the following equation:

$$\begin{Bmatrix} F_1 \\ F_2 \\ F_3 \end{Bmatrix} = \begin{bmatrix} K_{11} & K_{12} & K_{13} \\ K_{21} & K_{22} & K_{23} \\ K_{31} & K_{32} & K_{33} \end{bmatrix} \begin{Bmatrix} u_1 \\ u_2 \\ u_3 \end{Bmatrix} \quad \textbf{(2.17)}$$

where F_1 and u_1 correspond to the atoms at one end of the nanotube, the one that will be fixed. F_3 and u_3 are the atoms at the other end, where the force or the displacement will be applied, and F_2 and u_2 correspond to the majority of the atoms, which are between the two ends.

If a displacement is applied while fixing the other end, the forces will be unknown at both ends of the nanotube but they will be zero in between, the values of K will be as previously found and the displacement will be zero at the fixed end, unknown in the middle and a prescribed value at the other end (the value used here is 1). This is shown in the following equation:

$$\begin{Bmatrix} \overline{F_1} \\ \overline{0} \\ \overline{F_3} \end{Bmatrix} = \begin{bmatrix} \overline{\overline{K_{11}}} & \overline{\overline{K_{12}}} & \overline{\overline{K_{13}}} \\ \overline{\overline{K_{21}}} & \overline{\overline{K_{22}}} & \overline{\overline{K_{23}}} \\ \overline{\overline{K_{31}}} & \overline{\overline{K_{32}}} & \overline{\overline{K_{33}}} \end{bmatrix} \begin{Bmatrix} \overline{0} \\ \overline{u_2} \\ \overline{1} \end{Bmatrix} \quad \textbf{(2.18)}$$

Therefore there are three unknowns (F_1, F_3 and u_2) and a system of three equations can be solved as follows:

$$\overline{F_1} = \overline{\overline{k_{12}}} \cdot \overline{u_2} + \overline{\overline{k_{13}}} \cdot \overline{1} \quad \textbf{(2.19)}$$

$$\bar{0} = \overline{\overline{k_{22}}} \cdot \overline{u_2} + \overline{\overline{k_{23}}} \cdot \bar{1} \quad \textbf{(2.20)}$$

$$\overline{F_3} = \overline{\overline{k_{32}}} \cdot \overline{u_2} + \overline{\overline{k_{33}}} \cdot \bar{1} \quad \textbf{(2.21)}$$

From Eq 2.20,

$$\overline{\overline{u_2}} = -\overline{\overline{k_{22}}}^{-1} \cdot + \overline{\overline{k_{23}}} \cdot \bar{1} \quad \textbf{(2.22)}$$

And merging 2.21 and Eq 2.22,

$$\overline{F_3} = -\overline{\overline{k_{32}}} \cdot \left(\overline{\overline{k_{22}}}^{-1} \cdot + \overline{\overline{k_{23}}} \cdot \bar{1}\right) + \overline{\overline{k_{33}}} \cdot \bar{1} \quad \textbf{(2.23)}$$

where F_3 corresponds to a vector containing all the resulting forces at each atom. The sum of these forces is the total result of the applied displacement.

While writing the code for the explained steps, some problems were encountered. First, in most of the models generated, the nodes at the ends of the nanotube were not at the beginning and the end of the matrix. Although they were located in the upper and lower area of the matrix, they did not correspond to the first and last positions. Then, it is impossible to partition the stiffness matrix in a useful form.

To solve this problem, a new code that, instead of dividing the original matrix, creates new matrices taking selected rows and columns from the existing matrix (corresponding to the atoms at the ends) and placing them into the newly created matrices was needed. The number of the nodes located at the end could be easily found using GiD. However, the process to select and move all the rows and columns implied a high number of operations and therefore was inefficient.

A simpler procedure is to apply the displacement to the nanotube while changing the stiffness coefficients at the degrees of freedom where the displacement is applied to 1 along the principal diagonal of the stiffness matrix and setting all the cross terms to zero in each row and column that corresponds to a given degree of freedom where the displacement is applied, so that the resulting values of displacement are obtained to be the ones that we intended to apply after the solution of the system of equations.

The following lines will explain this efficient method. Two matrices are used to impose the boundary conditions of the nanotube. They are the following:

$$\begin{bmatrix} a_1 & \dots & a_n & b_1 & \dots & b_n \\ p_{1,1} & \cdots & & & \cdots & p_{1,2n} \\ \vdots & & & & & \vdots \\ p_{dof,1} & \cdots & & & \cdots & p_{dof,2n} \end{bmatrix} \quad \textbf{(2.24)}$$

$$\begin{bmatrix} a_1 & \dots & a_n & b_1 & \dots & b_n \\ f_{1,1} & \cdots & & & \cdots & f_{1,2n} \\ \vdots & & & & & \vdots \\ f_{dof,1} & \cdots & & & \cdots & f_{dof,2n} \end{bmatrix} \quad \textbf{(2.25)}$$

where a_i are the numbers of node of the atoms located at the first end of the nanotube and b_i correspond to the atoms at the other end. The subindex n denotes the number of atoms at each end and will depend on the diameter of the nanotube. The parameter $p_{i,j}$ will determine the condition of the atom and in the degree of freedom to which it corresponds. If it is 1, this node is fixed in this angle or direction, if it is 2 a force or moment is applied and if it is 0, any of the two other situations apply. Finally, $f_{i,j}$ denotes the magnitude of the force or moment to be applied at each degree of freedom and node.

As an example, the following matrices are used for a nanotube with a small diameter with the boundary conditions defined in Fig. 2.5.

$$\begin{bmatrix} 1 & 4 & 5 & 16 & 17 & 34 & 35 & 51 & 275 & 276 & 277 & 278 & 279 & 282 & 283 & 288 \\ 1 & 1 & 1 & 1 & 1 & 1 & 1 & 1 & 0 & 0 & 0 & 0 & 0 & 0 & 0 & 0 \\ 1 & 1 & 1 & 1 & 1 & 1 & 1 & 1 & 0 & 0 & 0 & 0 & 0 & 0 & 0 & 0 \\ 1 & 1 & 1 & 1 & 1 & 1 & 1 & 1 & 2 & 2 & 2 & 2 & 2 & 2 & 2 & 2 \\ 1 & 1 & 1 & 1 & 1 & 1 & 1 & 1 & 0 & 0 & 0 & 0 & 0 & 0 & 0 & 0 \\ 1 & 1 & 1 & 1 & 1 & 1 & 1 & 1 & 0 & 0 & 0 & 0 & 0 & 0 & 0 & 0 \\ 1 & 1 & 1 & 1 & 1 & 1 & 1 & 1 & 0 & 0 & 0 & 0 & 0 & 0 & 0 & 0 \end{bmatrix} \quad \textbf{(2.26)}$$

$$\begin{bmatrix} 1 & 4 & 5 & 16 & 17 & 34 & 35 & 51 & 275 & 276 & 277 & 278 & 279 & 282 & 283 & 288 \\ 0 & 0 & 0 & 0 & 0 & 0 & 0 & 0 & 0 & 0 & 0 & 0 & 0 & 0 & 0 & 0 \\ 0 & 0 & 0 & 0 & 0 & 0 & 0 & 0 & 0 & 0 & 0 & 0 & 0 & 0 & 0 & 0 \\ 0 & 0 & 0 & 0 & 0 & 0 & 0 & 0 & 1 & 1 & 1 & 1 & 1 & 1 & 1 & 1 \\ 0 & 0 & 0 & 0 & 0 & 0 & 0 & 0 & 0 & 0 & 0 & 0 & 0 & 0 & 0 & 0 \\ 0 & 0 & 0 & 0 & 0 & 0 & 0 & 0 & 0 & 0 & 0 & 0 & 0 & 0 & 0 & 0 \\ 0 & 0 & 0 & 0 & 0 & 0 & 0 & 0 & 0 & 0 & 0 & 0 & 0 & 0 & 0 & 0 \end{bmatrix} \quad \textbf{(2.27)}$$

In this example, only a unitary force has been applied in the axial direction of the nanotube. However, this method has the potential to apply forces to as many atoms as necessary. Furthermore, these forces can also be applied asymmetrically if it is needed.

At this point, and according to the described matrices, the stiffness matrix is modified (K*) and a loads vector (L) is created according to the forces to apply. Then the vector with the real displacements (u) can be found as:

$$\bar{u} = \overline{\overline{K^*}}^{-1} \bar{L} \quad \textbf{(2.28)}$$

Then, once the vector with the displacements is obtained, it can be substituted back to the unmodified system of equations, where the original stiffness matrix remains unmodified, and the resulting forces (F), called the reactions are obtained:

$$\bar{F} = \overline{\overline{K}} \cdot \bar{u} \quad \textbf{(2.29)}$$

The Young's modulus (Y) is the ratio of normal stress (σ) to normal strain (ε) obtained from a uni-axial tension test. It can be calculated as follows, according to Tserpes et al [26].

$$Y = {}^{\sigma}/_{\varepsilon} = {}^{F/A_0}\Big/_{u/L_0} \quad \textbf{(2.30)}$$

where F is the total force applied to the nanotube, A_0 is the cross-sectional area, L_0 is the initial length and u is the elongation due to the force. The value of F will correspond to the addition of the forces applied at each of the atoms at the ends of the nanotube. The cross-sectional area (A_0) equals π·D·t, where D is the diameter and t is the thickness. However, the thickness is considered unitary, as it is discussed in Section 4. Then,

$$Y = {}^{\sum F_i}\Big/_{\pi D(u/L_0)} \quad \textbf{(2.31)}$$

2.5 Creation of defects

The model developed is suitable to simulate effect of defects in the CNT structure. The defects are considered are those that result from missing carbon atoms. This is similar to breakage of bonds between atoms, which can be easily obtained by eliminating elements of the structure of the model.

The parameter that needs to be changed along the study is the percentage of defects due to broken bonds in a carbon nanotube. Hence, the first step is to determine how many bonds correspond to a percentage of defects. Then, a vector of randomized numbers with a normal distribution is generated; these numbers will correspond to the bonds to be eliminated. Then, the bonds (elements, in the structure mechanics model) are eliminated randomly and the remaining ones are renumbered.

At this point, the rest of the code can be executed as previously explained. It is necessary to repeat this process with different combinations of randomly generated bond breakages. The results are then studied statistically.

2.6 Simplified model

The model described in the previous sections considers that each node, corresponding to an atom, has six degrees of freedom. There are 3 directions of displacement and 3 angles of rotation. If the rotation angles of a node are not considered the model is considerably simplified. The effects on the accuracy of the results will be discussed in Section 4.

To do this reduction in the degrees of freedom, the stiffness matrix of the C-C bond must be modified. This matrix can be divided into four sub-matrices as shown in Eq. 2.4. These sub-matrices (see Eqs. 2.5, 2.6 and 2.7) will be modified as follows:

$$K_{ii} = \begin{bmatrix} EA/L & 0 & 0 \\ 0 & 12EI/L^3 & 0 \\ 0 & 0 & 12EI/L^3 \end{bmatrix} \quad \textbf{(2.32)}$$

$$K_{ij} = \begin{bmatrix} -EA/L & 0 & 0 \\ 0 & -12EI/L^3 & 0 \\ 0 & 0 & -12EI/L^3 \end{bmatrix} \quad \textbf{(2.33)}$$

$$K_{jj} = \begin{bmatrix} EA/L & 0 & 0 \\ 0 & 12EI/L^3 & 0 \\ 0 & 0 & 12EI/L^3 \end{bmatrix} \quad \textbf{(2.34)}$$

As the stiffness matrix of a bond between two carbon atoms has a reduced size (it is 6 x 6 instead of 12 x 12), the rotation matrix will also be reduced. Only the 6 first rows and columns will be used.

The rest of the code will not be affected by this change, though its execution will be faster due to the decreased size of the used variables.

2.7 Statistical data processing

The statistical characteristics of population of CNTs with defects are approximated by Monte Carlo simulations in which the model developed is used to obtain a relatively large number of results for each randomly distributed defect density as shown Table 3.5.

In the quality control of CNTs produced using direct tensile tests, an important question is how many tests should be carried out to accurately determine the mean value of CNT stiffness within a given confidence level. It may also be important to determine defect density accurately within a given confidence level. Once the testing program begins, the first operation performed with the obtained data is the arithmetic mean. This is the average value of all the Young's moduli that have been obtained from each test data. It is calculated as follows:

$$\overline{\boldsymbol{y}} = {}^{\boldsymbol{1}}\!/_{\boldsymbol{n}}\,(\boldsymbol{Y_1} + \boldsymbol{Y_2} + \boldsymbol{Y_3} + \ldots + \boldsymbol{Y_n}) \qquad \textbf{(2.35)}$$

where Y_i is the Young's modulus at i^{th} test and n is the number of results obtained.

The standard deviation of the results is also calculated. It is a measure of the variability of these results. It can be obtained as:

$$\boldsymbol{s} = \sqrt{\left((\boldsymbol{Y_1} - \overline{\boldsymbol{y}})^2 + (\boldsymbol{Y_2} - \overline{\boldsymbol{y}})^2 + (\boldsymbol{Y_3} - \overline{\boldsymbol{y}})^2 + \ldots + (\boldsymbol{Y_n} - \overline{\boldsymbol{y}})^2 \,/_{\boldsymbol{n-1}} \right)} \qquad \textbf{(2.36)}$$

For a small number of test results that form a sample of the population, the most suitable statistical distribution to use is the t-distribution. For a very large size sample, this distribution becomes the normal distribution.

To find the number of minimum tests, a random variable T is defined as:

$$\boldsymbol{T} = {}^{\sqrt{\boldsymbol{n}}(\overline{\boldsymbol{y}} - \boldsymbol{\mu})}\!/_{\boldsymbol{s}} \qquad \textbf{(2.37)}$$

where T has a t-distribution with n – 1 degrees of freedom. To test the hypothesis that μ equals a given value μ*, the test statistic to calculate is:

$$\boldsymbol{T = {\sqrt{n}(\bar{y} - \mu^{*})}/{s}} \quad \textbf{(2.38)}$$

This statistic will have a t-distribution with n – 1 degrees of freedom if the null hypothesis (that T lies in the interval [-a, a]) is true. The hypothesis is rejected at a 95% significance level if the calculated test statistic is outside the range from –a to a, where a is found from a t distribution table. Then:

$$\boldsymbol{Pr(-a < T < a) = 0.95} \quad \textbf{(2.39)}$$

Then for a given number of experimental tests (n), a 95% confidence interval for the mean Young's modulus will be:

$$\boldsymbol{\bar{y} \pm {as}/{\sqrt{n}}} \quad \textbf{(2.40)}$$

which can be derived from Eq. 2.38.

2.8 Analysis method

The following lines include a description of the analysis method used to calculate the Young's modulus of a carbon nanotube with a given percentage of defects. Each step was explained in detail in the previous sections. The complete code can be found in the Annex.

- Introduce data for:
  - Tube length
  - Tube diameter
  - Degrees of freedom
  - Prescripted displacement
  - C – C bond length
  - Percentage of imperfections
  - Number of iterations (when imperfections are present)
  - Force constants
- Transform variables to a non-dimensional space

- Introduce stiffness matrix for a single C – C bond
- Loop over the number of iterations
    - Load nanotube structure
    - Calculate number of defects from percentage
    - Loop over number of defects
        - Generate random number
        - Delete selected bond
    - Loop over number of elements
        - Find vector corresponding to the local axial direction
        - Find rotation angles
        - Assemble rotation matrix
        - Rotate bond stiffness matrix to global coordinates
        - Add contribution of element to global stiffness matrix
        - Set boundary conditions
        - Apply boundary conditions
        - Calculate applied displacements
        - Obtain resultant forces
        - Calculate mean displacements
        - Calculate total forces
        - Undo non-dimensional space changes in units
        - Calculate Young's modulus
        - Save Young's modulus (for statistical calculations, if imperfections are present)

3 RESULTS AND DISCUSSION

3.1 Nanotube model

The structural mechanics model developed is based on the known stiffness matrix of a carbon – carbon bond. As shown in section 1.2.3, the stiffness parameters EA, EI and GJ can be transformed into force constants. These force constants are known, as the C-C bond is also found in graphite sheets which have been extensively studied.

The force constants used, obtained from the work from Li et al. (2003) are $k_r/2$ = 469 kcal mol^{-1} $Å^{-2}$, $k_\theta/2$ = 63 kcal· mol^{-1} rad^{-2} and $k_\tau/2$=20 kcal mol^{-1} rad^{-2}. These units were transformed into the International System of units (SI) to be operated with the rest of magnitudes in the model which already were in this unit system. If the resulting values were expressed in nanometers, as found in some literature [26], they would be $k_r = 6.52 \cdot 10^{-7}$ N nm^{-1}, $k_\theta = 8.76 \cdot 10^{-10}$ N nm rad^{-2} and $k_\tau = 2.78 \cdot 10^{-10}$ N nm rad^{-2}. However, for the uniformity of the units inside the model and the agreement with the SI, length units should be in meters. After this change, the magnitude of the force constants changes as follows: k_r = 652 N m^{-1}, $k_\theta = 8.76 \cdot 10^{-19}$ N m rad^{-2} and $k_\tau = 2.78 \cdot 10^{-19}$ N m rad^{-2}.

The difference between the values of the force constants in the International System of units is extremely large (more than 20 orders of magnitude) and showed some problems during the computation process. In some cases, the variables with smaller values were wrongly considered zero. To overcome this problem the best solution found was to translate the values to a non-dimensional space prior to any calculation and undo this translation after the results were obtained.

The first option considered to be able to handle these force constants was to do the following dimensional change: [F] = k_r and [L] = L. Then, the resulting forces were multiplied by k_r and displacements by L to get forces in Newtons and displacements in meters. However, this option caused the matrix to be still nearly singular because of too small stiffness coefficients in the global system. Hence, a different characteristic quantity had to be chosen.

The alternative, which gave good results, was to use the following non-dimensional space [F] = k_θ/L^2 and [L] = L. Namely, the resulting forces were multiplied by k_θ/L^2 and displacements by L to get forces in Newtons and displacements in meters.

The present model has been originally designed to allow 6 degrees of freedom to each atom. Specifically, an atom can suffer displacements in the 3 directions

and rotation around the same 3 axes. This high number of degrees of freedom allows a higher accuracy but at a higher computational cost. With the objective of simplifying the model and reduction the size of the variables to use during the execution of the model, the degrees of freedom of an atom were reduced from six to three.

The analysis of the results showed that the variation of the results was reasonably small and that the computation time was reduced by almost 50%. This is caused by a weak effect of the torsional forces in a carbon nanotube when it is loaded axially. This conclusion was also reached by other researchers, who also stated the weak effect of the torsional force constant (k_T) in comparison with the others [13, 26].

Due to the computational advantages offered by the 3 degrees of freedom model and the small effects on the accuracy, this model has been used for the study of the effects of imperfections in CNT.

3.2 Young's modulus

Young's modulus has been calculated from the obtained stiffness matrix, as explained in section 2.4. In general, the Young's modulus can be defined by the following expression:

$$E = {}^{\sigma}/_{\varepsilon} = {}^{F/A_0}/_{\varepsilon} \qquad \textbf{(3.1)}$$

where E is the conventional Young's modulus, F is the sum of the applied forces, A_0 is the cross-sectional area and ε is the normal strain observed. For a cylindrical nanotube, the cross sectional area can be written as the diameter multiplied by the thickness and by pi ($\pi \cdot D \cdot t$).

However, there is not a consensus between researchers about the value of the thickness of a nanotube. The difference between values suggested can be up to 6 times which can cause serious confusion if the conventional form of Young's modulus shown in Eq. 3.1 is employed. The wide variety of wall thickness values used can be seen in Table 3.1.

To bypass this problem, some alternative definitions have been proposed such as the second derivative of the strain energy with respect to the axial strain per unit area of the nanotube [27] or per atom of the tube [28]. The form used in this work is known as surface Young's modulus (Y) and is related to the conventional form (E) as follows:

$$Y = E \cdot t \tag{3.2}$$

where t is the thickness of the nanotube walls.

Using this expression, the Young's modulus found for a zigzag nanotube with a diameter of 2.02 nm (i.e. with a chiral vector of (26,0)) and a length of 3.88 nm, is 332 TPa nm. The results for a zigzag nanotube with a smaller diameter were very similar. For a nanotube with a diameter of 1.01 nm (i.e. its chiral vector is (13, 0)) and the same length, the surface Young's modulus is 326 TPa nm.

The obtained results agree very well to other calculations found in the literature. At a first sight, these might seem quite different but they are due to the different wall thickness values used in the calculations. In order to properly compare them to the present results, the conventional Young's modulus has been converted to surface Young's modulus using the wall thickness from each investigation (see Table 3.1).

Table 3.1 Comparison of the surface Young's modulus obtained from different investigations.

Investigators	Method	Surface Young's modulus (TPa nm)	Wall thickness (nm)
Yakobson et al. [29]	Molecular dynamics	363	0.066
Zhou et al. [30]	Tight binding model	377	0.074
Kudin et al. [31]	Ab initio computations	343	0.089
Li et al. [13]	Structural mechanics	343	0.34
Lu et al. [32]	Molecular dynamics	332	0.34
Hernández et al. [27]	Molecular dynamics	416	-
Jin et al. [33]	Molecular dynamics	420	0.34
Chang et al. [15]	Molecular dynamics	360	-

Wu et al. [34]	Molecular dynamics	297	0.28
Tserpes et al. [26]	Structural mechanics	350	0.34
Present work	Structural mechanics	332	-

If the wall thickness values of Table 3.1 are analyzed, one can see that the value used by most of the researchers is 0.34 nm. This is the value corresponding to interlayer spacing of graphite.

As it was explained in the previous section, the model was adapted from six degrees of freedom to three in order to check if its efficiency was enhanced. The results of the Young's modulus for the same two zigzag carbon nanotubes are 319 TPa nm and 310 TPa nm for the diameters of 2.02 nm and 1.01 nm respectively.

The variation of the results due to the reduction in degrees of freedom is quite small (around 4%), so the simplified model can be used to obtain further results more efficiently.

3.3 Defects

Some defects have been introduced in the carbon nanotube structure in the form on broken atom bonds. These imperfections have a normal distribution, which is achieved using a random number generator from Matlab. Thirty iterations where necessary in order to obtain valid results as the elastic properties of the nanotube could change depending on the location or the concentration of the defects.

Table 3.2 shows the results of each of the iterations and each percentage of broken bonds. To extract conclusions and use the results the arithmetic mean and the standard deviation have been calculated and are shown in

Table 3.3 and Table 3.4.

Table 3.2 Young's modulus in TPa nm of all simulated nanotubes, for each percentage of defects.

Percentage of defects	1%	3%	5%	7.5%	10%	12.5%	15%
Nanotube 1	298.8	280.4	260.7	243.6	216.3	209.9	146.2

Nanotube 2	301.8	278.9	265.4	229.5	199.5	207.3	177.6
Nanotube 3	299.3	288.6	264.5	242.6	211.0	198.3	173.4
Nanotube 4	299.2	277.9	266.1	243.7	224.1	180.8	164.2
Nanotube 5	301.6	286.2	265.6	240.7	224.0	188.2	163.2
Nanotube 6	301.3	278.3	260.1	231.0	223.0	194.9	186.5
Nanotube 7	299.1	287.6	259.9	239.8	204.0	178.8	120.8
Nanotube 8	299.1	277.2	267.8	238.4	198.0	190.2	147.5
Nanotube 9	303.1	277.8	260.8	235.6	205.9	195.1	171.9
Nanotube 10	303.2	281.4	259.2	235.0	204.9	176.7	175.1
Nanotube 11	301.0	279.4	260.4	244.0	217.1	194.3	161.7
Nanotube 12	304.7	279.2	267.2	233.4	206.8	170.8	170.5
Nanotube 13	297.5	274.4	258.8	242.1	226.3	190.8	168.8
Nanotube 14	300.8	286.1	253.1	242.8	191.4	182.1	171.2
Nanotube 15	297.9	273.6	271.9	232.2	221.7	201.7	146.6
Nanotube 16	299.0	288.3	274.5	231.6	213.4	191.4	163.5
Nanotube 17	297.0	277.7	265.9	249.6	220.6	187.6	156.1
Nanotube 18	301.7	278.6	271.4	238.6	210.7	193.9	163.9
Nanotube 19	304.8	275.8	262.2	234.2	224.1	183.3	168.6
Nanotube 20	303.3	271.6	263.2	231.4	194.9	172.2	160.5
Nanotube 21	299.6	284.2	270.2	235.8	221.2	186.7	173.6
Nanotube 22	305.1	279.2	260.7	239.6	229.3	200.8	166.2
Nanotube 23	293.9	283.4	277.3	242.8	217.6	200.4	156.4
Nanotube 24	302.0	280.3	256.2	238.0	227.3	177.4	158.1
Nanotube 25	301.2	280.6	254.3	235.6	225.0	203.3	158.8
Nanotube 26	303.7	284.8	266.7	249.0	212.7	178.9	155.7
Nanotube 27	302.7	276.1	252.1	243.6	208.0	185.0	169.8
Nanotube 28	303.0	289.0	255.2	231.8	216.2	187.8	172.1
Nanotube 29	299.7	279.5	258.5	237.7	210.2	180.1	160.8
Nanotube 30	299.6	280.5	269.4	229.4	204.5	197.4	160.5

Table 3.3 Arithmetic means from the results shown in Table 3.2. Data is shown in Pa m.

Percentage of defects	**1%**	**3%**	**5%**	**7.5%**	**10%**	**12.5%**	**15%**
Arithmetic mean	300.8	280.5	263.3	238.1	213.6	189.5	163.0

As the number of broken bonds in a carbon nanotube increases, tensions cannot be well distributed along all the structure. The concentration of these tensions allows a higher deformation due to the applied force, which can be seen in the decreasing Young's modulus. The relation between the quantity of

imperfections in a nanotube and its Young's modulus is almost lineal, as can be seen in Fig. 3.1.

This would allow predicting Young's modulus of a nanotube if the percentage of defects is known. The opposite case is also possible, which is even more interesting. This could establish an approximate relationship between the elastic properties and the quantity of imperfections that could be used for quality testing of carbon nanotubes. Therefore, if a group of nanotubes are mechanically tested and, applying an axial force, the Young's modulus is obtained, the quantity of imperfections could be found, which would determine the quality of the nanotube.

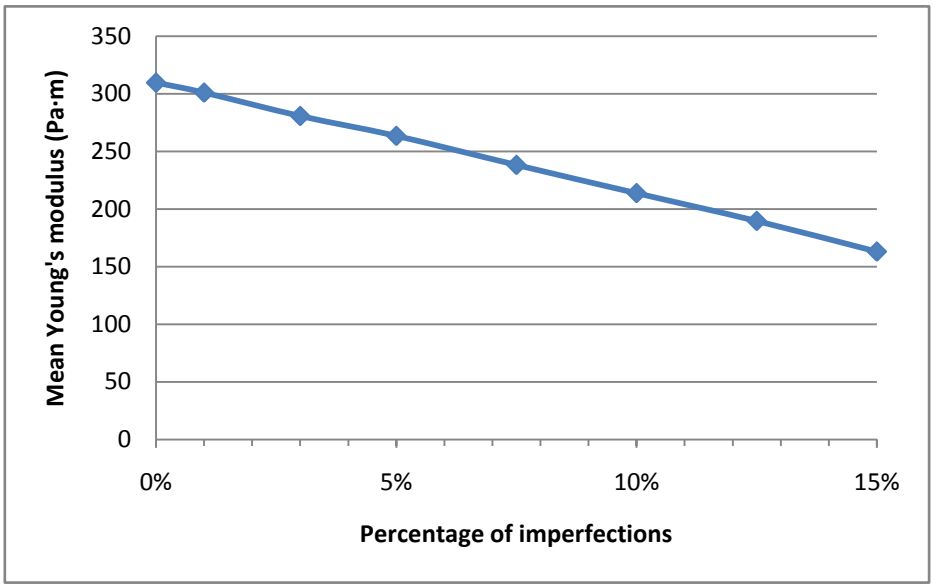

Fig. 3.1 Mean Young's modulus of the simulated CNT against their percentage of imperfections

The limitation of the data previously presented is that it can only be used with carbon nanotubes with a diameter near to 1 nm. For other diameters, the developed model could be used to extract results through the calculation of a stiffness matrix for the concrete case, though this is a slow process.

An alternative is to use the standard deviations of the results already available to predict the quality level of CNTs. They have been calculated from the data in Table 3.2 and are shown in Table 3.4.

Table 3.4 Standard deviation of the statistical results relating the Young's modulus and the percentage of imperfections (in Pa m)

Percentage of defects	1%	5%	10%	15%
Standard deviation	6.6	39.8	105.7	149.2

If the data in the previous table is plotted as in Fig. 3.2, it can be seen the clear relation between the standard deviation of the Young's modulus results and the percentage of imperfections in the nanotube. Although the linearity is not as clear as for the mean values of the Young's modulus good approximations can be obtained by interpolating between results. Therefore, a group of nanotubes of any diameter can be mechanically tested and if the standard deviation of their Young's modulus is obtained, it is possible to know an approximate value of their percentage of imperfections.

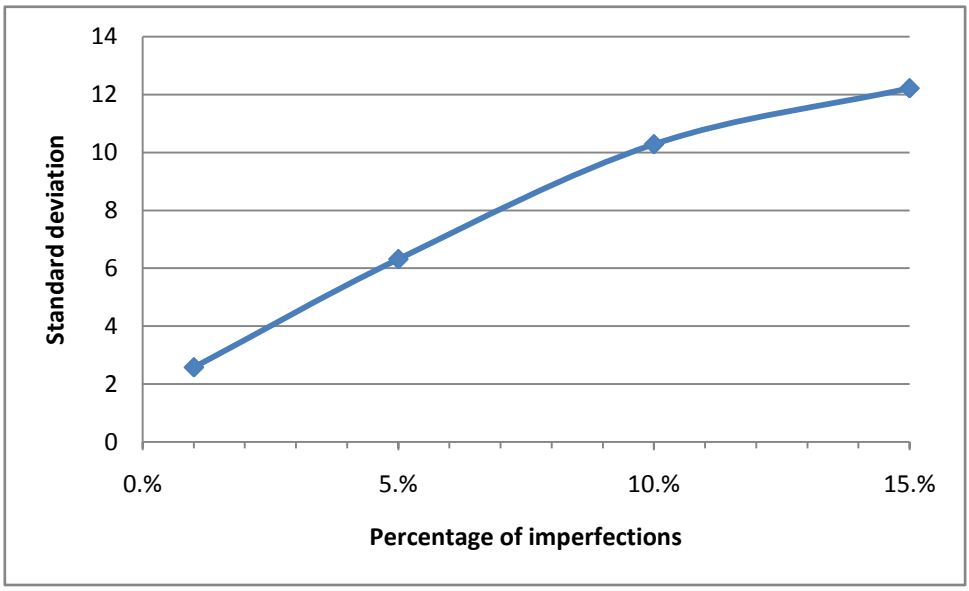

Fig. 3.2 Standard deviation of the Young's modulus of the simulated CNT against their percentage of imperfections

Experiments to estimate the mean value of stiffness and defect density of CNTs need a considerable amount of time and effort, so it is convenient to minimize the number of tests as much as possible.

Table 3.5 shows, for each sample of tests, the error obtained when the arithmetic mean is done. This has been calculated assuming a t distribution, as

explained in Section 2.7. As the standard deviation increases with the number of defects, more tests will be necessary to obtain results within the 95% confidence level. For example, considering that an error of 5% can be assumed, 3 tests will be necessary if the percentage of defects is 1% but up to 12 will be necessary if there are 15% defects.

Table 3.5 Percentage of error in the mean Young's modulus depending on the number of tests performed. For each percentage of defects, the percentage under 5% with the smallest number of tests is highlighted.

Number of tests	1% of defects	5% of defects	10% of defects	15% of defects
2	7.7%	21.5%	43.2%	67.3%
3	**2.1%**	6.0%	12.0%	18.6%
4	1.4%	**3.8%**	7.7%	11.9%
5	1.1%	3.0%	6.0%	9.3%
6	0.9%	2.5%	5.1%	7.9%
7	0.8%	2.2%	**4.5%**	6.9%
8	0.7%	2.0%	4.0%	6.3%
9	0.7%	1.8%	3.7%	5.8%
10	0.6%	1.7%	3.4%	5.4%
11	0.6%	1.6%	3.2%	5.0%
12	0.5%	1.5%	3.1%	**4.8%**
20	0.4%	1.1%	2.3%	3.5%
30	0.4%	1.1%	2.2%	3.4%
40	0.3%	0.8%	1.5%	2.4%
100	0.2%	0.5%	1.0%	1.5%

A standard deviation that corresponds to 5% of mean value may be assumed as it allows a reasonable accuracy without increasing excessively the number of necessary experiments for low values of defect density. As shown in Fig. 3.3, for nanotubes with a low quality (i.e. a high density of imperfections) the number of tests would be about 4 times higher if the standard deviation allowed were 2.5% instead of 5%.

To determine the defect density from a given batch of CNTs, one would carry out 3 tests and calculate the statistics of the results using the t-distribution as outlined in Section 2.7. However, since the defect density level can be anywhere between 1% (which requires a small number tests) and 15% (which requires a large number of tests), more test data is needed. Thus, in the subsequent tests, one would monitor the standard deviation to see if it stabilizes around a value or keeps changing. Once the standard deviation of the sample

stabilizes at a fixed value, the tests can be stopped. The standard deviation of the sample now could be compared to that of the population obtained by Monte Carlo simulations to estimate the defect density.

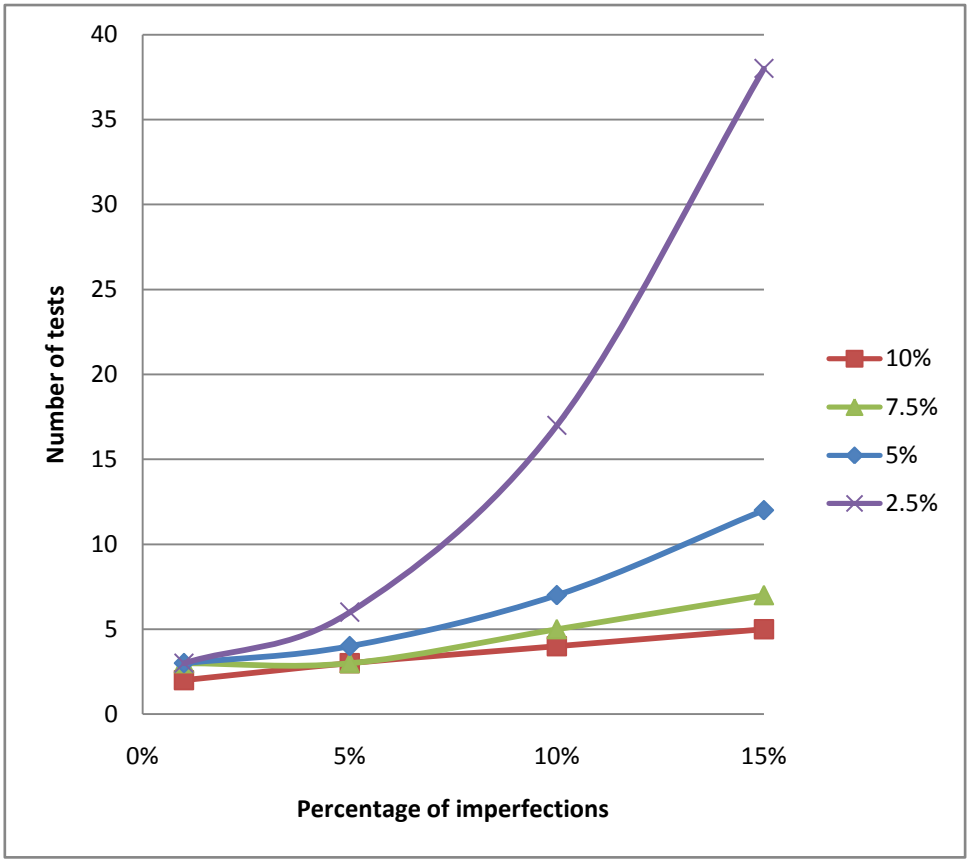

Fig. 3.3 Number of necessary tests against the number of imperfections to obtain results within the chosen margin of error. The curves are presented for different values of allowed standard deviation as a percentage of mean value.

4 CONCLUSIONS

During the last years, carbon nanotubes have been, from very different points of view, the center of numerous studies. Its exceptional mechanic properties allow very promising applications in a wide variety of fields. One of them is the aerospace sector, which can benefit from their very high strength and stiffness and yet low weight.

A method to analyze elastic properties has been developed. It is based in the analysis of a structure formed by nodes, representing the carbon atoms, and united by beam-like bonds. The stiffness matrix from a cylindrical beam is known and the mechanical parameters from this matrix are linked to the C – C bond through molecular dynamics. Each of the parameters is related to an energy term and thus to its force constant.

Once the stiffness matrix of a single bond has been obtained, it should be rotated and moved to be placed at its position in the carbon nanotube structure. This change from local to global coordinates should be made for each bond in a CNT. At the end of this process, a stiffness matrix corresponding to the elastic properties of a carbon nanotube will be obtained. To perform the assembly of each bond, a carbon nanotube was modeled with a meshing program which resulted in a list of the coordinates of each atom (nodes, in the model) and a connectivity matrix with the atoms connected by each bond (element, in the model).

When the stiffness matrix is ready, boundary conditions can be applied, according to the problem to solve. In this study, a deformation was applied to the nanotube in the axial direction and the resulting forces were read to calculate the Young's modulus. The values obtained have been compared to the ones existing in the literature, which were obtained through very different methods, and the results were similar to those previously available.

Two special considerations should be exposed about the developed model. Firstly, a considerable divergence in the thickness of a nanotube was found on previous works. Some of them calculated the surface Young's modulus to overcome this problem and obtain comparable parameters. This path was followed and the results were favorable. Secondly, once comparable results were obtained, the model was adapted from six to three degrees of freedom. The resulting model was simplified by not considering the torsion of the C – C bonds. The effects of torsional forces resulted to be very weak and the effects on the results were quite small while the computational time and necessary memory were considerably reduced. This simplification would allow, for example, testing nanotubes longer or with a larger diameter.

Then, the developed model has been used to study the effects of imperfections in the Young's modulus of a CNT. Different percentages of defects were created by deleting some of the bonds in the nanotube structure. The results showed that the Young's modulus is reduced linearly with the increase of the number of imperfections. This can be used to predict the percentage of defects of a group of nanotubes (i.e. their quality) according to their elastic properties, which can be measured experimentally.

The limitation of this method is that this would only apply to CNT with the same diameter of the present model. To overcome this, the standard deviation of the results obtained was calculated and a nearly-linear relation was also obtained. The advantage of the relation between the standard deviation of the Young's modulus and the number of defects is that it is not dependent on the diameter of the nanotube, so the applicability of the results is considerably broader.

The determination of minimum number of experiments necessary to obtain estimates of mean stiffness and defect density within a given confidence level (95%) has been described. It is important to minimize as much as possible the number of tests due to their cost. Assuming a t-distribution of the results, it has been shown that a few tests are sufficient for a low percentage of imperfections but it increases 3 times from 5% defect density to 15% defect density.

5 REFERENCES

[1] Kroto, H.W., Heath, J.R., O'Brien, S.C., Curl, R.F. and Smalley, R.E., "C60: Buckminsterfullerene", Nature, 318 (6042), 162-163 (1985).

[2] Kis, A., *Mechanical properties of mesoscopic objects*. École Polytechnique Fédérale de Lausanne (2003).

[3] Iijima, S., "Helical microtubules of graphitic carbon", Nature, 354 (6348), 56-58 (1991).

[4] Iijima, S., "High-Resolution Electron-Microscopy of Some Carbonaceous Materials", Journal of Microscopy, 99 (119), (1980).

[5] Lau, K., Chipara, M., Ling, H. and Hui, D., "On the effective elastic moduli of carbon nanotubes for nanocomposite structures", Composites Part B: Engineering, 35 (2), 95-101 (2004).

[6] Zhu, H.W., Xu, C.L., Wu, D.H., Wei, B.Q., Vajtai, R. and Ajayan, P.M., "Direct Synthesis of Long Single-Walled Carbon Nanotube Strands", Science, 296 (5569), 884-886 (2002).

[7] Saito, R., Dresselhaus, G. and Dresselhaus, M.S., *Physical properties of carbon nanotubes*, Imperial College Press, London, UK (1998).

[8] Reich, S., Thomsen, C. and Maultzsch, J., *Carbon nanotubes: basic concepts and physical properties*, Wiley-VCH, Weinheim, Germany (2004).

[9] Dai, L., "Radiation chemistry for microfabrication of conjugated polymers and carbon nanotubes", Radiation Physics and Chemistry, 62 (1), 55-68 (2001).

[10] Thostenson, E.T., Ren, Z. and Chou, T., "Advances in the science and technology of carbon nanotubes and their composites: a review", Composites Science and Technology, 61 (13), 1899-1912 (2001).

[11] Cadek, M., Coleman, J.N., Ryan, K.P., Nicolosi, V., Bister, G., Fonseca, A., Nagy, J.B., Szostak, K., Beguin, F. and Blau, W.J., "Reinforcement of Polymers with Carbon Nanotubes: The Role of Nanotube Surface Area", Nano Letters, 4 (2), 353-356 (2004).

[12] Xiao, J.R., Gama, B.A. and Gillespie, J., J.W., "An analytical molecular structural mechanics model for the mechanical properties of carbon nanotubes", International Journal of Solids and Structures, 42 (11-12), 3075-3092 (2005).

[13] Li, C. and Chou, T., "A structural mechanics approach for the analysis of carbon nanotubes", International Journal of Solids and Structures, 40 (10), 2487-2499 (2003).

[14] Gao, J., Itkis, M.E., Yu, A., Bekyarova, E., Zhao, B. and Haddon, R.C., "Continuous Spinning of a Single-Walled Carbon Nanotube−Nylon Composite Fiber", Journal of the American Chemical Society, 127 (11), 3847-3854 (2005).

[15] Chang, T. and Gao, H., "Size-dependent elastic properties of a single-walled carbon nanotube via a molecular mechanics model", Journal of the Mechanics and Physics of Solids, 51 (6), 1059-1074 (2003).

[16] Lau, K., Chipara, M., Ling, H. and Hui, D., "On the effective elastic moduli of carbon nanotubes for nanocomposite structures", Composites Part B: Engineering, 35 (2), 95-101 (2004).

[17] Zhu, Y., Ke, C. and Espinosa, H., "Experimental Techniques for the Mechanical Characterization of One-Dimensional Nanostructures", Experimental Mechanics, 47 (1), 7-24 (2007).

[18] Lau, K., Gu, C. and Hui, D., "A critical review on nanotube and nanotube/nanoclay related polymer composite materials", Composites Part B: Engineering, 37 (6), 425-436 (2006).

[19] Popov, V.N., Van Doren, V.E. and Balkanski, M., "Elastic properties of single-walled carbon nanotubes", Physical Review B, 61 (4), 3078 (2000).

[20] Goze, C., Vaccarini, L., Henrard, L., Bernier, P., Hemandez, E. and Rubio, A., "Elastic and mechanical properties of carbon nanotubes", Synthetic Metals, 103 (1-3), 2500-2501 (1999).

[21] Dalton, A.B., Collins, S., Munoz, E., Razal, J.M., Ebron, V.H., Ferraris, J.P., Coleman, J.N., Kim, B.G. and Baughman, R.H., "Super-tough carbon-nanotube fibres", Nature, 423 (6941), 703-703 (2003).

[22] Moniruzzaman, M. and Winey, K.I., "Polymer Nanocomposites Containing Carbon Nanotubes", Macromolecules, 39 (16), 5194-5205 (2006).

[23] Andrews, R., Jacques, D., Minot, M. and Rantell, T., "Fabrication of Carbon Multiwall Nanotube/Polymer Composites by Shear Mixing", Macromolecular Materials and Engineering, 287 (6), 395-403 (2002).

[24] Kashiwagi, T., Du, F., Douglas, J.F., Winey, K.I., Harris, R.H., and Shields, J.R., "Nanoparticle networks reduce the flammability of polymer nanocomposites", Nature Materials, 4 (12), 928-933 (2005).

[25] McCormac, J.C., Nelson, J.K., *Structural analysis : a classical and matrix methods approach*, Addison-Wesley, Reading, MA, USA (1997).

[26] Tserpes, K.I. and Papanikos, P., "Finite element modeling of single-walled carbon nanotubes", Composites Part B: Engineering, 36 (5), 468-477 (2005).

[27] Hernández, E., Goze, C., Bernier, P. and Rubio, A., "Elastic Properties of C and $B_xC_yN_z$ Composite Nanotubes", Physical Review Letters, 80 (20), 4502 (1998).

[28] Sánchez-Portal, D., Artacho, E., Soler, J.M., Rubio, A. and Ordejón, P., "Ab initio structural, elastic, and vibrational properties of carbon nanotubes", Physical Review B, 59 (19), 12678 (1999).

[29] Yakobson, B.I., Brabec, C.J. and Bernholc, J., "Nanomechanics of Carbon Tubes: Instabilities beyond Linear Response", Physical Review Letters, 76 (14), 2511 (1996).

[30] Xin, Z., Jianjun, Z. and Zhong-can, O., "Strain energy and Young's modulus of single-wall carbon nanotubes calculated from electronic energy-band theory", Physical Review B, 62 (20), 13692 (2000).

[31] Kudin, K.N., Scuseria, G.E. and Yakobson, B.I., "C_2F, BN, and C nanoshell elasticity from ab initio computations", Physical Review B, 64 (23), 235406 (2001).

[32] Lu, J.P., "Elastic Properties of Carbon Nanotubes and Nanoropes", Physical Review Letters, 79 (7), 1297 (1997).

[33] Jin, Y. and Yuan, F.G., "Simulation of elastic properties of single-walled carbon nanotubes", Composites Science and Technology, 63 (11), 1507-1515 (2003).

[34] Wu, Y., Zhang, X., Leung, A.Y.T. and Zhong, W., "An energy-equivalent model on studying the mechanical properties of single-walled carbon nanotubes", Thin-Walled Structures, 44 (6), 667-676 (2006).

6 ANNEX

The Matlab code used in the analysis is given below. It is for analyzing a CNT with a diameter of 1.01 nm, a length of 3.38 nm, having 1% imperfection distributed randomly and with deformation applied in the axial direction. Only 3 degrees of freedom at each node (or atom) have been considered.

```
clc
clear all
% Initial data:
TubeLength = 3.38e-9;        %m
TubeDiameter = 1.011e-9;     %m
dof = 3;                     %degrees of freedom at each node
presc_disp=1e-9;             %m
L=0.141e-9;                  %m Length of a C-C bond
numIterations=1;            %number of iterations
numNaN=0;
% Force constants from Tserpes et al. (2005):
            % EA=6.52e-7  %N·nm^-1
            % EI=8.76e-10 %N·nm·rad^-2
            % GJ=2.78e-10 %N·nm·rad^-2
EA=L*652;  %N
EI=L*8.76e-19; %N·m^2·rad^-2
GJ=L*2.78e-19; %N·m^2·rad^-2
% Transformation to nondimensional space:
    % [F]=EI/L^2; [L]=L. Then, multiply the resulting forces with
    % EI/L^2 and displacements with L to get forces in MN and
    % displacements in nm.
Lreal=L;
EIreal=EI;
presc_disp_real=presc_disp;
EA=EA/EI*L^2;
GJ=GJ/EI;
presc_disp=presc_disp/L;
L=1;
EI=1;
% Stiffness matrix of a C-C bond (adapted to 3 DOF):
KBond=[EA/L    0      0        -EA/L   0       0   ;
        0 12*EI/L^3   0        0  -12*EI/L^3   0   ;
        0      0 12*EI/L^3     0       0 -12*EI/L^3;
     -EA/L     0      0        EA/L    0       0   ;
        0 -12*EI/L^3  0        0   12*EI/L^3   0   ;
        0     0 -12*EI/L^3     0       0  12*EI/L^3];

% Calculations:
it=1;
while it<numIterations+1
    load elements1s.mat
    load nodes1s.mat
    nNodes = 494;
    nElements = 728;
    nodesDef=zeros(1,nNodes);
    % Defects:
    defectsPercentage=1;    %per cent
    numDef=round((nElements*defectsPercentage)/100);
    for i=1:numDef
```

```
        def=round((nElements-1)*rand)+1;    %The addition of 1 and -1
is to avoid zero as the resulting random number.
elements(def,:)=[];
        nElements=nElements-1;
    end

    k=zeros(nNodes*dof,nNodes*dof);
    zeroMatrix = [0 0 0; 0 0 0; 0 0 0];

    vi = [1 0 0];
    vj = [0 1 0];
    vk = [0 0 1];

    for i=1:nElements
        n = elements(i,1);
        m = elements(i,2);
        localZ = [nodes(m,1)-nodes(n,1), nodes(m,2)-nodes(n,2),
nodes(m,3)-nodes(n,3)];
        localZ = localZ/sqrt(localZ*localZ');

    %     Find local y
        if not(localZ(3)==0)
           y3 = (-localZ(1)-2*localZ(2))/localZ(3);
           localY = [1 2 y3];
        elseif not(localZ(2)==0)
           y2 = (-localZ(1)-2*localZ(3))/localZ(2);
           localY = [1 y2 2];
        elseif not(localZ(1)==0)
           y1 = (-localZ(2)-2*localZ(3))/localZ(1);
           localY = [y1 1 2];
        end

        localY = localY/sqrt(localY*localY');

    %     Find local z
        localX = cross(localY, localZ);
        localX = localX/sqrt(localX*localX');

    %     Values for rotation matrix
        cosZI = localZ*vi';
        cosZJ = localZ*vj';
        cosZK = localZ*vk';
        cosYI = localY*vi';
        cosYJ = localY*vj';
        cosYK = localY*vk';
        cosXI = localX*vi';
        cosXJ = localX*vj';
        cosXK = localX*vk';

        rotationSmall = [
            cosZI cosZJ cosZK;
            cosYI cosYJ cosYK;
            cosXI cosXJ cosXK
                 ];



        RR = [
            rotationSmall zeroMatrix;
```

```
            zeroMatrix rotationSmall];

        KElement = RR'*KBond*RR;

        n = elements(i,1);
        m = elements(i,2);
        k((n-1)*dof+1:n*dof,(n-1)*dof+1:n*dof)=k((n-1)*dof+1:n*dof,
(n-1)*dof+1:n*dof)+KElement(1:dof, 1:dof);
        k((m-1)*dof+1:m*dof,(m-1)*dof+1:m*dof)=k((m-1)*dof+1:m*dof,
(m-1)*dof+1:m*dof)+KElement(dof+1:dof*2, dof+1:dof*2);
        k((n-1)*dof+1:n*dof,(m-1)*dof+1:m*dof)=k((n-1)*dof+1:n*dof,
(m-1)*dof+1:m*dof)+KElement(1:dof, dof+1:dof*2);
        k((m-1)*dof+1:m*dof,(n-1)*dof+1:n*dof)=k((m-1)*dof+1:m*dof,
(n-1)*dof+1:n*dof)+KElement(dof+1:dof*2, 1:dof);
    end

    head = [1 4 5 16 17 34 35 51 52 72 73 86 87   476 477 478 479 482
483 488 489 490 491 492 493 494;
         1 1 1 1 1 1 1 1 1 1 1 1 1  0 0 0 0 0 0 0 0 0 0 0 0 ;
         1 1 1 1 1 1 1 1 1 1 1 1 1  0 0 0 0 0 0 0 0 0 0 0 0 ;
         1 1 1 1 1 1 1 1 1 1 1 1 1  2 2 2 2 2 2 2 2 2 2 2 2
         ];
    fload = [1 4 5 16 17 34 35 51 52 72 73 86 87   476 477 478 479 482
483 488 489 490 491 492 493 494;
         0 0 0 0 0 0 0 0 0 0 0 0 0  0 0 0 0 0 0 0 0 0 0 0 0 ;
         0 0 0 0 0 0 0 0 0 0 0 0 0  0 0 0 0 0 0 0 0 0 0 0 0 ;
         0 0 0 0 0 0 0 0 0 0 0 0 0  1 1 1 1 1 1 1 1 1 1 1 1
         ]*presc_disp;

    save k_real.mat k;
    loads=zeros(1,dof*nNodes);
    for i=1:size(head(1,:),2)
      for j=1:dof
        if head(j+1,i)~=0 % displacement prescribed
          for m=1:dof*nNodes
              loads(m)=loads(m)-k(m,(head(1,i)-1)*dof+j)*fload(j+1,i);
          end
          k((head(1,i)-1)*dof+j,:)=zeros(1,dof*nNodes);
          k(:,(head(1,i)-1)*dof+j)=zeros(dof*nNodes,1);
          k((head(1,i)-1)*dof+j,(head(1,i)-1)*dof+j)=1.0;
          loads(1,(head(1,i)-1)*dof+j)=fload(j+1,i);
          if fload(j+1,i) ~= 0
              kdof=j;
          end
          else % force prescribed
              loads(1,(head(1,i)-1)*dof+j)=fload(j+1,i);
              if fload(j+1,i) ~= 0
                  kdof=j;
              end
        end
      end
    end

    clear RR KEelement;
    clear elements;
    disps=loads/k;
    clear k;
    load k_real.mat
    forces=k*disps';
    clear k
```

```
    tip=[476 477 478 479 482 483 488 489 490 491 492 493 494];
    % 'tip'contains the node numbers at one tip
    avdisp=0;
    for i=1:size(tip,2)
        tip_disps(i)=disps((tip(i)-1)*dof+kdof);
        avdisp=avdisp+disps((tip(i)-1)*dof+kdof);
    end
    fixed=[1 4 5 16 17 34 35 51 52 72 73 86 87];
    % 'fixed'contains the node numbers at the other tip
    totforce=0;
    for i=1:size(tip,2)
        totforce=totforce+forces((tip(i)-1)*dof+kdof);
    end
    avdisp=avdisp/size(tip,2);
    avdisp=avdisp*Lreal; % in meters
    tip_disps=tip_disps*Lreal; % in meters
    totforce = totforce * EIreal/Lreal^2; % in Newtons
    YY=totforce/(TubeDiameter*avdisp/TubeLength*pi) % N/m=Pa*m
    Young(it)=YY;
    it=it+1;
end
```